frontiers in Chemistry

TYPE Review
PUBLISHED 17 November 2026
DOI 10.3389/fchem.2026.1985198

Check for updates

OPEN ACCESS

EDITED BY
Bowen Yao,
Nanjing University of Science and Technology, China

REVIEWED BY
Resmond Lat Reaño,
University of the Philippines Los Baños, Philippines
Birendra Kumar,
Hemchand Yadav University, India

*CORRESPONDENCE
Fatih Ciftci,
faciftcii@gmail.com,
fciftci@fsm.edu.tr
Javad Rahebi,
cevatrahebi@topkapi.edu.tr

RECEIVED 01 September 2026
REVISED 23 October 2026
ACCEPTED 29 October 2026
PUBLISHED 17 November 2026

CITATION
Akkad H, Ciftci F, Özerol EA and Rahebi J (2026) Carbon- and polymer-integrated colloidal systems for biosensing: interfacial mechanisms, performance trade-offs, and applications. *Front. Chem.* 14:1985198. doi: 10.3389/fchem.2026.1985198

COPYRIGHT
© 2026 Akkad, Ciftci, Özerol and Rahebi. This is an open-access article distributed under the terms of the Creative Commons Attribution License (CC BY). The use, distribution or reproduction in other forums is permitted, provided the original author(s) and the copyright owner(s) are credited and that the original publication in this journal is cited, in accordance with accepted academic practice. No use, distribution or reproduction is permitted which does not comply with these terms.

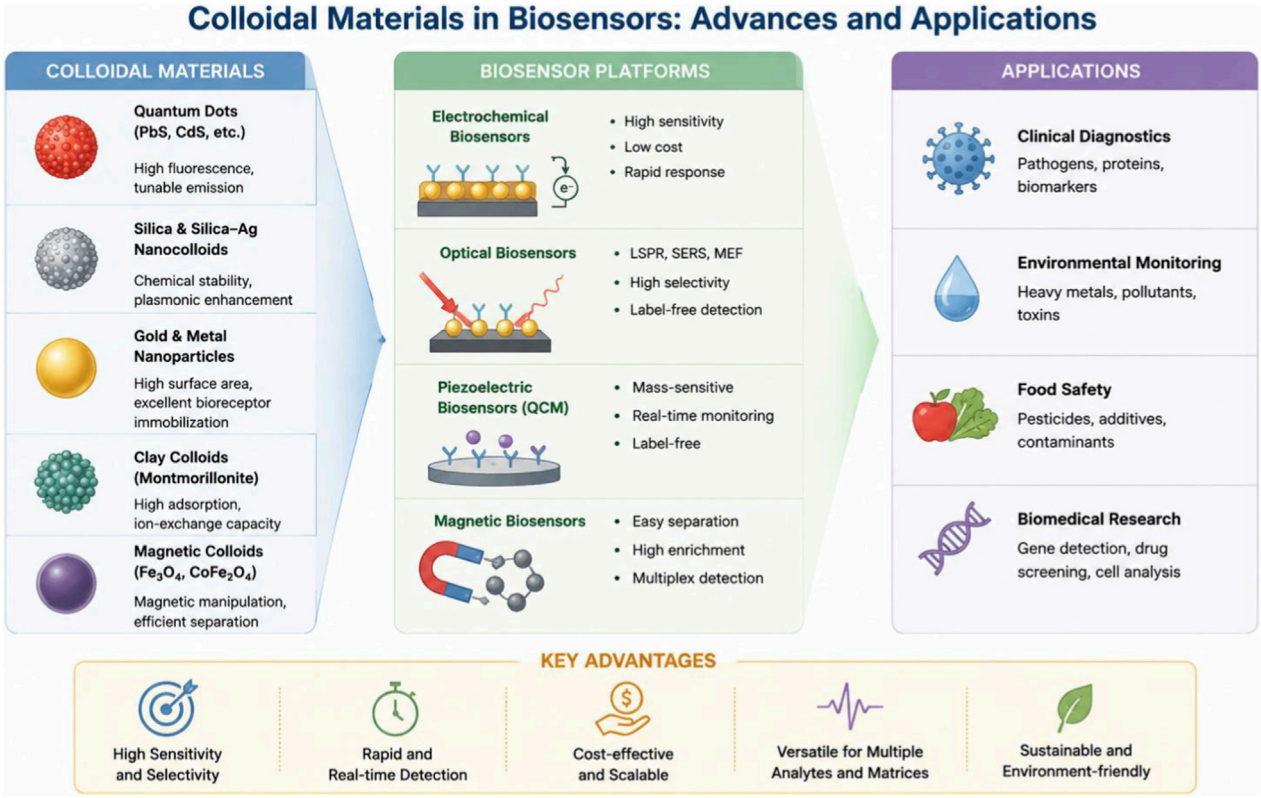
Carbon- and polymer-integrated colloidal systems for biosensing: interfacial mechanisms, performance trade-offs, and applications

Haya Akkad[1], Fatih Ciftci[2,3,4]*, Esma Ahlatcıoğlu Özerol[1] and Javad Rahebi[5]*

[1]Department of Bioengineering, Faculty of Chemical and Metallurgical Engineering, Yildiz Technical University, Istanbul, Türkiye, [2]Faculty of Engineering, Department of Biomedical Engineering, Fatih Sultan Mehmet Vakıf University, Istanbul, Türkiye, [3]BioriginAI Research Group, Department of Biomedical Engineering, Fatih Sultan Mehmet Vakıf University, Istanbul, Türkiye, [4]Biomedical Electronic Design Application and Research Center (BETAM), Fatih Sultan Mehmet Vakıf University, Istanbul, Türkiye, [5]Department of Electrical and Electronics Engineering, Istanbul Topkapi University, Istanbul, Türkiye

Colloidal nanoparticles integrated with carbonaceous supports and polymeric matrices provide tunable interfaces for biosensing, but their analytical benefits depend on how hybridization affects charge transfer, analyte transport, receptor accessibility, and stability. In this review, we summarize the fundamental principles of electrochemical, optical, and piezoelectric biosensors, and we examine the functional contributions of colloids to signal amplification, selective biorecognition, and advanced interface engineering. We emphasize the growing demand for rapid, sensitive analytical systems in applications such as medical diagnostics, food safety, environmental monitoring, and point-of-care testing. We reviewed major classes of colloidal materials, including metallic nanoparticles, quantum dots, silica colloids, and clay-based structures such as montmorillonite, with respect to their physicochemical advantages and biosensor performance. Integrated analyses of colloid-enriched electrochemical, optical, piezoelectric, and magnetic platforms reveal both the promising aspects and limitations of current technologies. Despite their strengths, practical application remains hampered by issues such as particle aggregation, long-term instability, inconsistent immobilization onto sensor substrates, and fabrication challenges in hybrid or nanoscale systems. Recent advances, such as engineered miniprotein receptors, quantum dot-based electrochemical sensing, and fiber-based metal-enhanced fluorescence (MEF) structures, illustrate emerging strategies to overcome these limitations. This review concludes that future progress will rely on atomic-scale surface engineering, scalable and reproducible fabrication methods, non-enzymatic recognition motifs, and the integration of colloidal materials with smart biointerfaces. Overall, colloids represent a rapidly developing class of materials with the potential to advance biosensor technologies toward more accurate, durable, and accessible platforms for biomedical, environmental, and industrial applications.

KEYWORDS
biomedical, biosensor, colloidal material, environment, food safety



GRAPHICAL ABSTRACT

Highlights

- Colloidal materials significantly enhance sensitivity and signal amplification in biosensor platforms.
- Metallic, silica, quantum dot colloids enable versatile electrochemical and optical sensing.
- Colloid surface functionalization improves biorecognition efficiency and analytical selectivity performance.
- Hybrid colloidal nanostructures address stability, reproducibility, and fabrication challenges effectively.
- Colloid-based biosensors advance point-of-care diagnostics and environmental monitoring applications.

1 Introduction

Biosensing technologies have undergone a significant transformation in recent decades, fuelled by growing needs in clinical diagnostics, environmental monitoring, food safety, and personalized medicine (Akkad et al., 2026; Akkad and Ahlatcıoğlu Özerol, 2026; Sreejith et al., 2023; Li et al., 2023). These needs have driven researchers to develop devices that enable rapid, sensitive, selective, and minimally invasive detection of a broad range of biological and chemical analytes (Heydari and Haghayegh, 2014). In this context, colloid-based materials have become some of the most effective and adaptable components for enhancing biosensor platforms. Colloidal particles in the micro-to nanoscale range possess unique physicochemical properties that differ significantly from those of their bulk counterparts. Their high surface-to-volume ratio, customizable size and shape, controllable optical and electronic properties, and versatile surface functionalization capabilities make them particularly well-suited for interfacing with biological systems. Various colloidal materials drive innovations in biosensing. Table 1 summarizes the colloidal materials used in biosensors. Metallic nanoparticles such as gold, silver, and platinum enhance optical and electrochemical sensing through surface plasmon resonance, catalytic activity, and efficient electron transfer (Heydari and Haghayegh, 2014; Li et al., 2023). Semiconductor colloids, including quantum dots and metal oxides, can provide size-dependent fluorescence, photostability, and intense light–matter interactions, which are essential for imaging and optoelectronic biosensors. Polymeric colloids offer biocompatible, durable platforms for biomolecule immobilization, drug delivery, and signal modulation (Fu et al., 2024). Silica colloids enable high loading of enzymes, antibodies, and nucleic acids due to their porosity and adjustable surface properties (Heydari and Haghayegh, 2014; Kuntoji et al., 2024). Clay colloids, such as montmorillonite, provide ion-exchange, mechanical reinforcement, and hybrid interfaces that enhance sensor durability. Incorporating colloids into biosensors increases recognition and transduction by promoting selective target binding and amplifying signals via optical, catalytic, or

TABLE 1 A summary of colloids used in biosensors.

System/ Target	Comparison	Reported result	Critical interpretation	Refs.
Gold/graphite–PPy or PANI/Glucose	Polymer identity and polymerization duration	PPy provided 1.35-fold higher sensitivity and 2.57-fold lower LOD than PANI. Increasing PPy polymerization from 22 to 68 h extended the linear-range upper limit from 19.9 to 49.3 mM, while sensitivity decreased from 59.4 to 5.83 μA mM^{-1} cm^{-2}	Demonstrates a polymer-dependent **sensitivity–working-range trade-off**. Polymerization time does not directly establish film thickness	Wu et al. (2018)
AuNP–PPy–rGO/ Glucose	Analytical evaluation of a ternary multilayer interface	5.6 μM LOD and 0.2–8 mM linear range	Demonstrates carbon/polymer/gold integration. The complete sensor's LOD alone does not quantify each component's contribution	Mubarakali et al. (2023)
CuO–graphene/ ITO/Glucose	Analytical evaluation of the assembled hybrid	1 μM LOD and 1610 μA mM^{-1} cm^{-2} sensitivity	Initial performance does not establish graphene-mediated protection or superiority over enzymatic sensors tested under different conditions	Devi et al. (2012)
Au–PPy/Pt/ Xanthine	Initial performance versus combined use/storage endpoint	0.4 μM LOD, 0.4–100 μM range, 4 s response; approximately 60% activity retained after 200 uses over 100 days, stored at 4 °C	Provides quantitative durability evidence. Activity loss does not identify its mechanism; repeated uses are not regeneration cycles	Yun et al. (2019)
AuNP-modified QCM/SEA	Nanostructured versus planar surfaces; direct versus sandwich assay	Direct-assay LOD decreased from 20 to 8 ng mL^{-1}; sandwich detection reached approximately 1 ng mL^{-1} within 25 min	Supports improved recognition at nanostructured interfaces. Additional sandwich amplification must be distinguished from the surface modification itself	Al-Gethami et al. (2022)
Ag@SiO_2–PCL/ Fluorescence assay	Fibrous versus glass support; Ag-containing versus Ag-free fibers	Greater protein loading than glass and higher fluorescence than SiO_2–PCL controls	Controls distinguish the structural contribution of PCL from Ag-mediated optical enhancement; no unverified numerical enhancement factor is assigned	
$CoFe_2O_4$/Ca-alginate QCM/ Pb(II)	Composite versus $CoFe_2O_4$-only coating	Frequency shifts: 25.85 versus 27.49 Hz at 25 °C; 33.87 versus 23.63 Hz at 35 °C, respectively	Alginate produced a temperature-dependent effect. Larger frequency shifts do not alone demonstrate lower LOD; this is a chemical-sensor reference.	Carvalho et al. (2022)

electrochemical properties. This results in lower detection limits, faster responses, and improved stability. In biomedicine, these advancements support earlier diagnoses, point-of-care testing, real-time monitoring, and reliable detection of pathogens, nucleic acids, metabolites, and biomarkers (Heydari and Haghayegh, 2014; Li et al., 2023; Kuntoji et al., 2024).

Previous reviews have examined macromolecule–nanoparticle hybrids for biosensing, including conjugated polymers and macrocyclic systems used for signal amplification, as exemplified by Kuntoji et al. The contribution of the present review is a complementary interface-centered synthesis of colloid–carbon, colloid–polymer, and ternary hybrid architectures. Its central question is how integration into a sensing interface preserves, modifies, or compromises the functional properties of the colloidal phase. Accordingly, the review examines the relationship between interfacial organization and electrical connectivity, analyte accessibility, receptor presentation, signal generation, and stability. This approach emphasizes the evidence required to attribute a performance improvement to hybridization rather than to differences in material loading, assay conditions, or signal-processing procedures (Shanbhag et al., 2023).

This review focuses on colloidal nanoparticles integrated with carbonaceous supports, polymeric matrices, or both. Colloid–carbon and colloid–polymer architectures are considered alongside ternary colloid–carbon–polymer systems; the presence of all three components is therefore not an inclusion requirement. We examine these architectures by the function of each constituent: the colloidal phase provides catalytic, optical, magnetic, or recognition-related functionality, while the carbonaceous and polymeric components regulate electrical connectivity, particle immobilization, interfacial accessibility, and the local sensing environment. Single-component colloidal platforms are retained as reference cases for assessing the benefits and limitations of hybridization. Across electrochemical, optical, and piezoelectric/magnetic platforms, the discussion links material composition and integration methods to signal transduction, analytical performance, stability, and fabrication constraints.

TABLE 2 Overview of colloidal materials in electrochemical biosensors.

Colloidal material	Sensor target	Mechanism/Sensor architecture	Performance highlights	References
Latex microspheres + colloidal Au/Ag	Proteins, DNA, biomolecules	Dielectrophoretic assembly of microspheres between electrodes; immunoactive latex binding; Au tagging with Ag enhancement	Disposable on-chip arrays; high sensitivity; direct conductivity readout	Devi et al. (2012)
Flower-shaped CuO nanoparticles	Glucose (non-enzymatic)	CuO nanoparticles integrated with graphene on ITO; improved electro-oxidation; characterized by XRD, UV–Vis, TEM, SEM	LOD 1 μM; sensitivity 1610 μA mM^{-1} cm^{-2}; linear range 1–850 μM; stable and fast response	Velev and Kaler (1999)
Au–polypyrrole (AuPPy) colloids	Xanthine	XOD enzyme immobilized on AuPPy–Pt electrode; Au enhances electron transfer	LOD 0.4 μM; linear range 0.4–100 μM; 4 s response; effective for meat sample analysis	Xu et al. (2010)
Gold colloids (Hb–Au–carbon paste)	Nitric oxide (NO)	Hb adsorbed on Au-colloid-modified paste, enabling direct electron transfer and mediator-free NO reduction	LOD 1×10^{-7} M; linear 9×10^{-7}–3×10^{-4} M; high stability and selectivity	Lei et al. (1996)
Montmorillonite colloid + methylene Blue N	Hydrogen peroxide (H_2O_2)	HRP + NMBN co-immobilized in montmorillonite hydrogel on GCE	Linear 5 μM–2.2 mM; LOD 6×10^{-7} M; excellent mediator stability	Zhao et al. (2024)
PbS colloidal quantum dots	SARS-CoV-2 spike protein	Engineered miniprotein LCB binds to spike; interaction is detected on a CQD-based electrochemical chip	LOD: 3.31 pg mL^{-1} with the three-electrode system and 9.58 fg mL^{-1} with the HEMT device.	Lau et al. (2017)
Gold nanoparticles (AuNP)	Plant pathogen DNA	RPA amplification + AuNP-enhanced DPV on SPCE strip	~10^4× more sensitive than PCR; 60 min detection; suitable for early infection monitoring	Soundharraj et al. (2021)

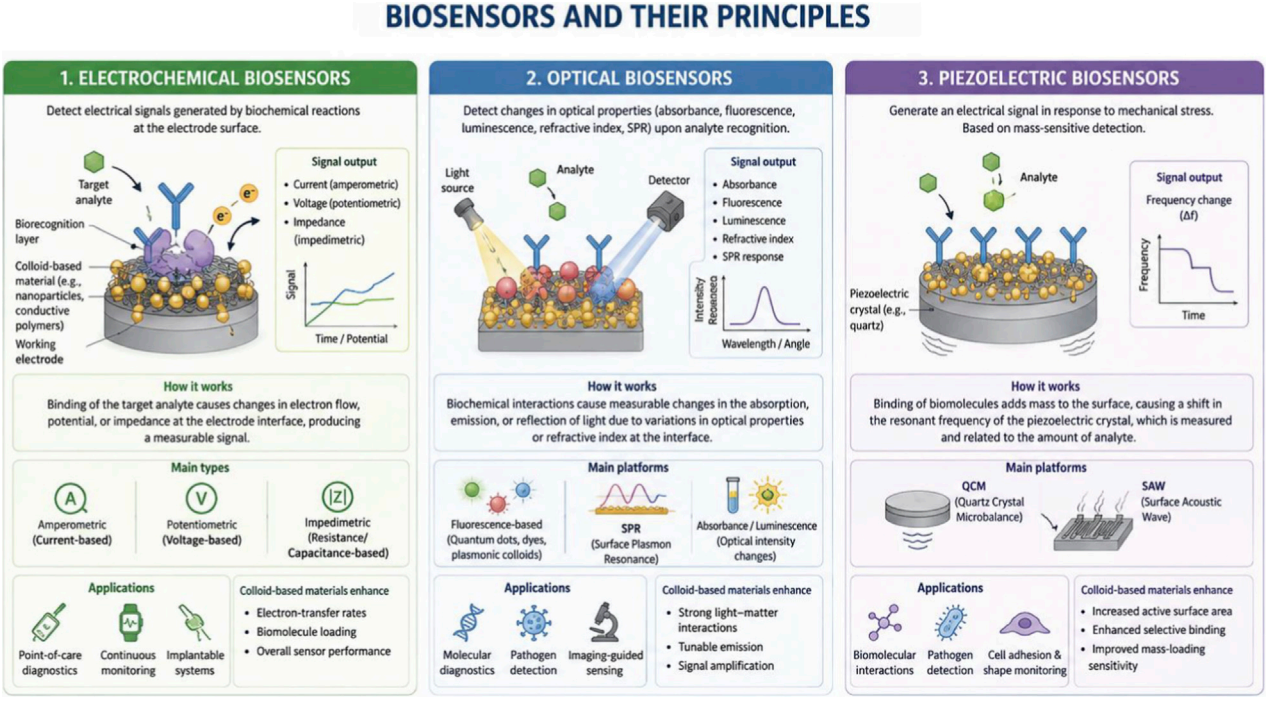


FIGURE 1
Biosensors and their types.

2 Biosensors and their principles

Biosensors couple a biological recognition element with a transducer that converts target recognition into a measurable signal. This review considers electrochemical, optical, and piezoelectric/magnetic platforms, emphasizing how colloidal particles and their carbonaceous or polymeric partners influence the recognition–transduction interface. The principal transduction categories are summarized in Figure 1.

2.1 Electrochemical biosensors

Electrochemical biosensors monitor changes in current, potential, or impedance associated with a recognition event or a coupled biochemical reaction. In colloidal hybrid electrodes, the measured response depends on electrical connectivity, receptor immobilization, accessible reaction sites, and analyte transport (Naresh and Lee, 2021; Simoska et al., 2020). Consequently, increased current or decreased impedance must be interpreted alongside appropriate controls before being attributed to improved electron-transfer kinetics (Kress et al., 2014). Table 2 provides an overview of colloidal materials used in electrochemical biosensors.

2.2 Optical biosensors

Optical biosensors detect recognition-dependent changes in absorption, emission, scattering, refractive index, or Raman signals. Colloidal particles can act as dispersed reporters or as components of immobilized optical interfaces. Their performance depends on particle organization, spectral properties, receptor presentation, and interactions with surrounding coatings or scaffolds (Damborský et al., 2016), (Swain et al., 2023).

2.3 Piezoelectric biosensors

Piezoelectric biosensors monitor changes in acoustic resonance following interactions at a functionalized surface. In QCM measurements, the response can reflect captured material together with coupled solvent and the mechanical properties of the sensing layer. Nanoparticle and polymer coatings must therefore be evaluated for their effects on both target recognition and acoustic coupling (Li et al., 2023; Skládal, 2024; Pan et al., 2024).

3 Colloids

Colloids are small particles (ranging from 1 to 1000 nm) evenly dispersed throughout another substance, much like particles suspended in a liquid. Because their size is between dissolved molecules and larger particles, they do not settle rapidly, making them highly stable and capable of interacting intensively with biological molecules (Heydari and Haghayegh, 2014; Shukla et al., 2022).

Colloidal materials have specific physicochemical characteristics distinct from those of other materials, making them highly attractive for biosensor development. Their nanoscale dimensions provide a high surface-area-to-volume ratio, enabling the immobilization of biomolecular recognition elements such as antibodies, nucleic acids, or enzymes, many of which possess numerous active sites (Heydari and Haghayegh, 2014). Such a high surface area-to-volume ratio would be expected to maximize target-analyte encounters, resulting in higher detection efficiencies. In addition to possessing high surface area, colloids have adjustable optical, electrical, and magnetic properties that are dependent on their particle composition and structure. Metallic nanoparticles, such as gold and silver, exhibit strong light absorption and scattering, whereas semiconductor quantum dots exhibit size-tunable fluorescence (Damborský et al., 2016; Geng et al., 2022).

These tunability features significantly improve signal sensitivity and lower the detection limit across various biosensing platforms. Colloidal stability is another key factor for sensor performance. Proper surface functionalization or polymer coatings prevent nonspecific aggregation, ensuring a consistent size distribution of colloids across physiological and analytical conditions. This stability also enhances sensor reproducibility and long-term operational dependability. Moreover, colloidally stable systems are highly adaptable, as their particle surfaces can be functionalized to facilitate selective, intense interactions with specific biological targets. Through controlled functionalization techniques, colloids can be customized to detect a wide range of analytes, supporting the development of biosensors with high specificity and versatility for clinical diagnostics, environmental monitoring, and food safety applications (Shukla et al., 2022).

3.1 Types of colloidal materials

Metal colloidal nanoparticles are dispersed systems with nanoscale metallic cores, prepared with controlled size, shape, and surface chemistry. Their properties differ from bulk metals, featuring high surface-to-volume ratios, quantum electronic characteristics, and optical responses that make them crucial in biosensors (Gutiérrez-Santana et al., 2024; Zhao et al., 2008). Synthesizing them in colloidal form offers stable, functional surfaces for biomolecular interactions, which are essential for signal generation in various sensors. A key feature is their extreme sensitivity to changes in size and shape, influencing band structure, surface energy, electron density, and photon-electron interactions (Gutiérrez-Santana et al., 2024; Zhao et al., 2008). In plasmonic metals such as gold, silver, and copper, surface plasmon resonance (SPR) creates characteristic absorption bands, enabling uses ranging from colorimetric detection to sensitive localized surface plasmon resonance (LSPR) sensors. Their electronic conductivity aids electron transfer, boosting electrochemical sensitivity. Gold and silver nanoparticles on electrodes enhance signals and facilitate controlled biomolecular interactions through binding, electrostatics, thiol-gold bonds, or polyelectrolyte layers (Gutiérrez-Santana et al., 2024; Zhao et al., 2008). The following subsections discuss gold, silver, copper/copper oxide, zinc oxide, semiconductor quantum dots, silica, and montmorillonite.

3.1.1 Gold nanoparticles (AuNPs)

Gold nanoparticles are among the most extensively studied metallic colloids and are considered a widely investigated

material in biomedical applications. This recognition stems from gold's chemical inertness, biocompatibility, and surface chemistry, which make it well-suited to controlled functionalization. Dispersed AuNPs exhibit localized surface plasmon resonance. Aggregation can modify interparticle plasmonic coupling, producing changes in the absorption spectrum and visible colour (Ben Haddada et al., 2018). SPR is a critical mechanism for optical signal amplification in diagnostic sensors. Furthermore, the gold surface exhibits high affinity for molecules containing thiol groups (–SH), amines ($–NH_2$), or thioethers. Therefore, immobilizing DNA, aptamers, antibodies, peptides, or drug molecules onto the AuNP surface is straightforward Figure 2 illustrates fluorescence enhancement in SiO_2–AgNP nanocomposites (Malathi et al., 2022). AuNPs are widely used in biosensors for applications such as surface-enhanced Raman scattering (SERS), electrochemical signal amplification, color-change-based lateral flow assays, and target biomolecule detection. They are also being evaluated as robust light-to-heat converters for local heating of tumor tissues in photothermal therapy (Song et al., 2021).

3.1.2 Silver nanoparticles (AgNPs)

Silver nanoparticles are among the most widely used metallic colloids, especially for their antibacterial properties. The strong interaction of Ag^+ ions with biological membranes and the production of reactive oxygen species (ROS) give silver a unique role in biological systems. Surface plasmon resonance is also observed in AgNPs, but they exhibit a sharper, more intense SPR band than gold. This feature makes AgNPs highly beneficial in SERS-based detection systems; silver is even more effective than gold at boosting Raman signals. Silver's antibacterial effect is based on three main mechanisms: disruption of the cell membrane by silver ions, inhibition of DNA replication, and oxidative stress caused by ROS formation. As a result, they are ideal for wound dressings, antimicrobial coatings, and biosensor surfaces. AgNPs are frequently used in color-changing chemical sensors, SERS substrates, electrochemical detection platforms, and antimicrobial biomaterial composites. However, controlling dosage is crucial in biomedical uses due to the risk of long-term toxicity (Zhang et al., 2024; Jhuang et al., 2021).

3.1.3 Copper and copper oxide nanoparticles (Cu and CuO NPs)

Copper is a valuable, low-cost plasmonic material because it is a much more economical metal than gold and silver. Both Cu and CuO nanoparticles offer a wide range of functional applications. Copper nanoparticles can also exhibit surface plasmon resonance, making them attractive in low-cost SERS and color-change analysis platforms. However, a significant drawback of CuNPs is their tendency to oxidize. Therefore, they must be coated with polymers, proteins, or organic ligands to increase stability. CuO is a semiconductor metal oxide. Thanks to its optoelectronic properties, it is widely used in electrochemical sensors, glucose oxidase-free glucose sensors, and catalytic biosensors. Both copper and copper oxide possess potent antimicrobial activity. They exert a multifaceted biological effect through cellular membrane damage, ion release, and oxidative stress mechanisms. Cu/CuO nanoparticles offer low-cost, effective nanomaterials for biosensor electrode modifications, environmental analyses, antibacterial coatings, and photocatalytic applications (Ramesh et al., 2022).

3.1.4 Zinc oxide nanoparticles (ZnO NPs)

ZnO is one of the most researched metal oxide nanoparticles in the biosensor field. Its wide band gap (3.37 eV), high exciton binding energy, and ease of synthesis make ZnO attractive for both electronic and biological devices. ZnO has a semiconductor structure and interacts strongly with UV light. It can be produced in various morphologies, such as nanorods, nanoflowers, and nanotubes, which facilitate analyte binding by increasing surface area. ZnO nanoparticles can generate ROS under certain conditions, and this property is being utilized in antimicrobial biomaterials. The biological effects of ZnO depend on dose, dissolution, surface chemistry, and exposure conditions; Zn^{2+} release can contribute to cytotoxicity (Zhang et al., 2024).

3.1.5 Quantum dots (QDs)

Colloidal quantum dots are semiconductor nanocrystals usually measuring between 2 and 20 nm. Their key feature is the ability to adjust the band gap and electronic energy levels based on nanocrystal size, a physical phenomenon called quantum confinement. This tunability is the main reason for the broad range of quantum dots' uses, including photodetectors, biosensors, imaging systems, and solar cells. Quantum dots produced in colloidal solutions are stabilized with organic ligands, which both passivate surface defects and maintain colloidal stability. This enables the nanocrystals to remain dispersed in solution for long periods and facilitates their incorporation into biological or optoelectronic structures (Ma et al., 2015).

3.1.6 Silica colloids

Silica (SiO_2) colloids are inorganic nanoparticles that have found wide application in nanotechnology due to their easy synthesis, chemical stability, large surface area, and rich surface chemistry. While SiO_2 particles alone provide a stable, low-toxicity, and processable platform, the resulting SiO_2 –Ag core–shell or core–compatible structures, when hybridized with the optical or catalytic advantages of metallic nanoparticles (especially Ag), provide versatile properties, particularly in optical (SERS, LSPR, MEF) and electrochemical biosensor designs. Silica is generally regarded as biocompatible; however, caution must be exercised regarding the potential for respiratory exposure or *in vivo* accumulation in nanoparticle form. The toxicity of AgNPs depends on the release of ions and particle size. Consequently, conducting comprehensive *in vitro* and *in vivo* toxicological evaluations (such as MTT, hemolysis, ROS assay, and histology) is imperative for any device or nanomaterial. Coating strategies, including a complete SiO_2 shell, poly (ethylene glycol) (PEG), or protein coatings, have proven effective in mitigating toxicity (Chapter 1 General chemistry of, 1979).

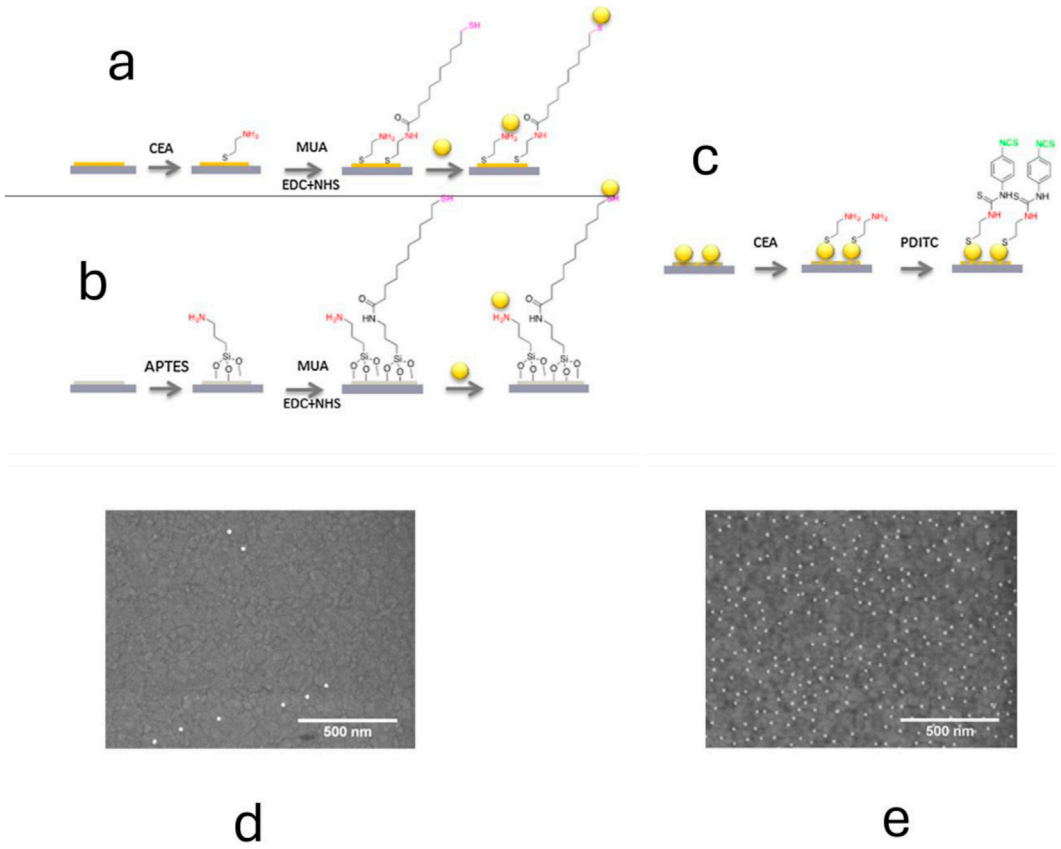


FIGURE 2
Three schematics and two scanning electron micrographs show gold nanoparticle immobilization and surface functionalization on quartz crystal sensors. (**a**) shows treatment of a gold-coated sensor with cysteamine (CEA) and 11-mercaptoundecanoic acid (MUA) before nanoparticle attachment. (**b**) shows a corresponding route for a silicon-coated sensor using APTES and MUA. (**c**) shows further functionalization of immobilized nanoparticles with CEA and PDITC. Scheme 1 of Ben Haddada et al. (2018). (**d**) shows a few bright particles on the gold-coated surface, while (**e**) shows more numerous bright particles across the silicon-coated surface.

3.1.7 Montmorillonite clay colloids

Montmorillonite-based clay-mineral colloids are natural nanostructured systems vital in biomaterials science and environmental technology due to their layered structure, high surface area, and ion-exchange capacity. As a member of the smectite group, it has a 2:1 layered crystal structure with an octahedral alumina layer between two tetrahedral silica layers, allowing water and ions to penetrate. This makes the mineral swellable, dynamic, and environmentally responsive. Its negative charge and exchangeable cations enable binding of organic molecules, proteins, pharmaceuticals, and metal ions via electrostatic or hydrogen-bonding interactions, thereby benefiting controlled release, adsorption, and the development of biocompatible materials. Its nanometer-scale layers enhance interactions with polymers, boosting mechanical, thermal, and barrier properties. In biomedicine, thanks to low cytotoxicity and high adsorption, it supports moisture regulation in wound dressings, carries antibacterial agents, immobilizes enzymes, or guides cell behavior. It is also essential in sustainable biomaterials because it is natural, abundant, and environmentally friendly. Its adjustable interlayer spacing and surface chemistry make it a versatile colloidal platform for various applications. Montmorillonite aids biosensors by safely immobilizing enzymes, DNA, or proteins on surfaces without disrupting their structure, maintaining activity longer. In electrochemical sensors, it accelerates electron transfer and enhances surface performance when combined with polymers such as poly (vinyl alcohol) (PVA), chitosan, polyaniline (PANI), and polypyrrole (PPy), thereby offering conductivity and mechanical stability. For environmental sensors that detect heavy metals and pollutants, montmorillonite's adsorption capacity quickly captures toxic substances such as Pb^{2+}, Cd^{2+}, and organic dyes, thereby lowering detection limits. In optical and SERS sensors, it prevents metal nanoparticle aggregation, creating stable "hot spot" regions that enhance Raman signals and device stability (German et al., 2022). Figure 3 summarizes colloids commonly used in biosensors.

3.2 Carbonaceous components in colloidal hybrid interfaces

Carbonaceous components in colloidal hybrid interfaces serve distinct functions depending on their dimensionality, surface chemistry, and electrical properties. Graphene-derived sheets and carbon nanotubes can provide pathways connecting nanoparticles to the underlying electrode, whereas carbon dots may function

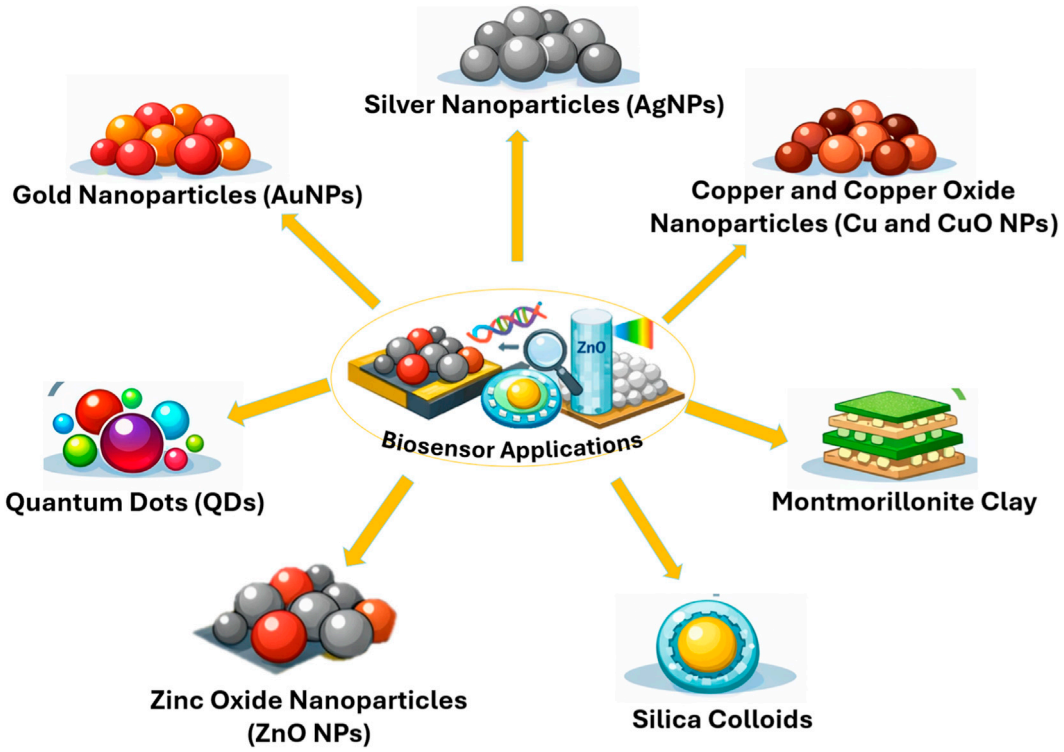


FIGURE 3
Schematic representation of the main classes of colloidal materials used in the development of biosensor platforms.

primarily as optical reporters. Carbon paste provides a conductive composite support into which colloidal particles and bioreceptors can be incorporated. These materials should therefore be evaluated according to their specific contribution to the sensing architecture rather than treated as interchangeable sources of increased surface area.

Graphene, graphene oxide (GO), and reduced graphene oxide (rGO) illustrate the balance between electrical connectivity and chemical functionalization. The conjugated structure of graphene supports electrical conduction, while the oxygen-containing groups of GO provide sites for nanoparticle attachment and biomolecule coupling but disrupt its electronic network. Partial reduction can restore conductivity while retaining some functional groups; however, the resulting properties depend on the reduction conditions and residual defects. In a comparative study of carbon-supported AuNPs, the carbon derivative influenced nanoparticle morphology, dispersion, stability, and localized surface plasmon resonance, demonstrating that support selection can affect both interfacial organization and optical response (Wang et al., 2009). Consequently, rGO should not automatically be considered superior to GO: an electrochemical interface may prioritize electrical connectivity, whereas a receptor-bearing or optical interface may benefit from a different balance of functionalization and dispersion.

Carbon nanotubes provide an alternative, one-dimensional framework for constructing interconnected nanoparticle-containing films. Their integration with colloids can distribute catalytic or recognition sites throughout a conductive network. For example, a glucose biosensor was fabricated using layer-by-layer assembled carbon nanotube/chitosan/AuNP films, combining a carbon framework with a polymeric immobilization matrix and a nanoparticle component (Wang et al., 2018). Nevertheless, nanotube bundling, nonuniform deposition, and excessive functionalization can compromise the accessibility or electrical continuity of the interface. The relevant design variables therefore include nanotube dispersion, nanoparticle loading, and the amount of polymer required to maintain film integrity without obstructing analyte transport.

Carbon dots and graphene quantum dots require a different interpretation because their contribution may be photophysical rather than predominantly conductive. In colloidal optical assays, their fluorescence can be modulated by interactions with metallic nanoparticles. A fluorescent aptasensor for acetamiprid, for example, exploited the inner filter effect between AuNPs and carbon dots (Liu and Ju, 2003). Such architectures demonstrate that carbon–colloid integration can regulate optical readout without forming a continuous conducting network. However, fluorescence attenuation should not automatically be assigned to electron transfer or Förster resonance energy transfer; absorption overlap, fluorescence lifetime, and appropriate optical controls are needed to distinguish possible mechanisms.

Carbon paste electrodes constitute a separate support category rather than a discrete carbon nanomaterial. Their particulate carbon–binder structure allows colloids and biological recognition elements to be incorporated into a renewable sensing surface. A hemoglobin/colloidal-gold carbon paste electrode has

been reported for reagentless nitrite detection, illustrating this integration strategy (Carvalho et al., 2022). Its performance nevertheless depends on the carbon-to-binder ratio, modifier distribution, and accessibility of the incorporated components. Across these carbon-containing architectures, evidence of a hybridization benefit requires comparison with the corresponding carbon-only and colloid-only interfaces under matched conditions.

3.2.1 Graphene, graphene oxide, and reduced graphene oxide

Graphene-based materials provide two-dimensional supports for integrating colloidal nanoparticles into sensing interfaces. Their contribution depends on the balance between electrical connectivity, surface functionalization, and particle accessibility. Graphene possesses an extended conjugated carbon network, whereas graphene oxide (GO) contains oxygen-bearing groups that facilitate aqueous processing and provide sites for nanoparticle attachment and biomolecule coupling. However, oxidation disrupts electronic conjugation and reduces conductivity. Reduced graphene oxide (rGO) partially restores the conductive network while retaining residual functional groups and defects. Consequently, graphene, GO, and rGO should not be treated as interchangeable supports (Wang et al., 2009).

Colloidal nanoparticles can be combined with these sheets through adsorption, chemical coupling, or growth on the carbon surface. In electrochemical architectures, the carbon component can connect spatially distributed catalytic particles to the electrode; in optical systems, it can influence particle distribution and the local optical environment. A comparative investigation of AuNPs supported by graphene-derived materials examined differences in nanoparticle morphology, dispersion, stability, and localized surface plasmon resonance, illustrating the importance of support chemistry (Wang et al., 2009).

The same interactions that promote nanoparticle attachment can introduce limitations. Sheet restacking reduces accessible surface area, while excessive particle loading can obstruct recognition sites or produce heterogeneous aggregates. Furthermore, increased conductivity after GO reduction may be accompanied by fewer functional groups and poorer aqueous dispersibility. Material selection should therefore reflect the intended transduction mechanism rather than an assumption that greater reduction necessarily improves sensing. Demonstrating a hybridization benefit requires matched carbon-only, nanoparticle-only, and hybrid controls, together with characterization of particle coverage and carbon oxidation state.

3.2.2 Carbon nanotubes

Carbon nanotubes (CNTs) provide one-dimensional frameworks for constructing interconnected colloidal sensing films. Their principal contribution is the formation of electrical pathways between nanoparticle-containing regions and the underlying electrode. Surface functionalization can additionally introduce attachment sites for nanoparticles, polymers, and biological recognition elements. Depending on the fabrication route, nanoparticles may be immobilized on previously dispersed CNTs, grown on their surfaces, or incorporated together with CNTs into a polymeric matrix.

A representative ternary architecture was demonstrated using layer-by-layer assembled CNT/chitosan/AuNP films on a glassy carbon electrode, followed by glucose oxidase immobilization within a crosslinked chitosan matrix (Wang et al., 2018). This configuration combines a carbon framework, a nanoparticle component, and a film-forming polymer. The components perform complementary functions: CNTs contribute to electrical connectivity, AuNPs provide additional electrochemically active interfaces, and chitosan supports film assembly and enzyme immobilization. However, the response of the complete sensor does not independently quantify the contribution of each constituent.

CNT integration also introduces a dispersion–connectivity trade-off. Bundling can produce nonuniform coatings and inaccessible internal surfaces, whereas aggressive oxidation may introduce defects that alter electrical transport. Dispersants and polymer coatings can improve processing but may separate neighboring nanotubes or obstruct nanoparticle surfaces. Accordingly, CNT loading, functionalization, and polymer content should be optimized together. Relevant evidence includes comparisons with CNT-free and nanoparticle-free interfaces, coating reproducibility, and measurements that distinguish increased electroactive area from changes in interfacial kinetics (Wang et al., 2018).

3.2.3 Carbon dots and graphene quantum dots

Carbon dots (CDs) and graphene quantum dots (GQDs) extend carbon–colloid integration beyond conductive electrode supports. Carbon dots constitute a heterogeneous family of nanoscale carbon-based emitters, whereas GQDs comprise small graphene domains with properties influenced by lateral dimensions, edge structure, and surface chemistry. Their optical response may involve both conjugated domains and surface-associated states; fluorescence should therefore not be attributed exclusively to quantum confinement. Neither material should be confused with semiconductor colloidal quantum dots such as PbS.

In optical biosensors, CDs and GQDs can serve as fluorescent reporters coupled to metallic nanoparticles through recognition-dependent changes in optical interaction or spatial separation. An acetamiprid aptasensor combined fluorescent CDs with AuNPs and exploited the inner filter effect to regulate fluorescence (L et al., 2022). In another aptasensing architecture, target binding released GQDs from AuNP-associated assemblies, restoring fluorescence for the detection of phthalic acid esters (Liu and Ju, 2003). These examples demonstrate distinct functions for the carbon and metallic components: the carbon-based dots supply the fluorescent output, while the AuNP-containing assembly modulates that output in conjunction with molecular recognition.

Mechanistic interpretation remains essential. Fluorescence attenuation can result from excitation or emission absorption, energy transfer, electron transfer, or aggregation, and these processes cannot be distinguished from intensity measurements alone. Absorption spectra, fluorescence lifetimes, and suitable separation controls are therefore important. Additional limitations include synthesis-dependent surface chemistry,

heterogeneous emissive populations, and changes in response with pH or sample composition. Comparisons should assess batch consistency and matrix effects rather than assuming that incorporation of a carbon-based emitter necessarily improves selectivity or analytical sensitivity.

3.2.4 Carbon paste supports

Carbon paste electrodes represent a composite support category rather than a distinct carbon nanomaterial. Conventional formulations contain conductive carbon particles dispersed in a binder, commonly a nonconducting liquid. Colloidal particles and biological recognition elements can be incorporated into the paste or immobilized on its exposed surface. The resulting interface combines a conductive carbon network with a processable matrix, allowing surface renewal and adjustment of the modifier composition.

A hemoglobin/colloidal-gold carbon paste electrode has been reported for reagentless nitrite detection based on the direct electrochemistry of the immobilized protein (German et al., 2022). In this architecture, the carbon paste supplies the electrode framework, while the gold-containing interface supports integration of the protein with the conductive phase. Nevertheless, demonstrating protein electrochemistry at the complete interface does not establish that every incorporated nanoparticle participates in electron transfer. Comparisons with hemoglobin-containing paste without gold and gold-containing paste without hemoglobin are needed to distinguish the component contributions.

Performance depends on carbon-to-binder ratio, modifier distribution, wetting, and contact between conductive particles. Excess binder can restrict electrical connectivity or analyte access, whereas uneven colloid incorporation can generate surface-to-surface variability. Renewal of the paste may also expose different proportions of nanoparticles and bioreceptors. Consequently, preparation reproducibility, component retention, and repeated surface renewal should be evaluated alongside detection limits. Carbon paste supports are therefore useful integration matrices, but their processing flexibility must be balanced against the need for a chemically and electrically reproducible sensing surface.

3.3 Polymeric components in colloidal hybrid interfaces

Polymeric components should be selected according to the limitation they are intended to address in a colloidal sensing interface. Depending on their chemistry and organization, polymers can retain nanoparticles, immobilize bioreceptors, regulate permeability, or provide a mechanically coherent scaffold. Conducting polymers may additionally participate in electrical transduction, whereas nonconducting matrices mainly control the physical and chemical sensing environment. Polymer incorporation is therefore not intrinsically beneficial: improved particle retention or receptor immobilization may be accompanied by reduced electrical access, slower diffusion, or changes in the measured optical or acoustic response.

Conducting polymers such as polypyrrole (PPy) and polyaniline (PANI) can combine an immobilization matrix with an electronically active phase. Their performance nevertheless depends on oxidation state, doping, operating pH, and film formation conditions. A comparative glucose-biosensor study using dendritic gold-modified graphite electrodes found that the PPy-containing configuration was 1.35 times more sensitive and exhibited a 2.57 times lower detection limit than the corresponding PANI configuration (Vaid et al., 1995). Increasing polymerization duration also decreased sensitivity in both systems. These findings demonstrate that polymer identity and deposition conditions influence analytical performance, rather than merely providing a protective coating. Because polymerization duration can alter several film characteristics simultaneously, its effect should not be attributed exclusively to thickness without direct structural measurements.

Hydrophilic biopolymers such as chitosan provide a different function. Their film-forming properties and reactive groups facilitate the assembly of nanoparticle-containing layers and the immobilization of biological recognition elements. In the carbon nanotube/chitosan/AuNP glucose-sensing architecture discussed above, chitosan provided a matrix for constructing the multilayer interface and immobilizing glucose oxidase (Wang et al., 2018). However, chitosan is not intrinsically electronically conductive, and its protonation, swelling, and permeability depend on the surrounding medium. Its concentration and crosslinking should therefore be optimized to retain the sensing components while preserving electrical connections and analyte accessibility.

Ion-selective polymer coatings can instead address interference from electroactive sample constituents. Nafion, a negatively charged ionomer, has been used to restrict access by anionic interferents, including ascorbate and urate, in glucose enzyme electrodes (Yang et al., 2025). More recently, a multienzyme creatinine biosensor combined AuNP-modified screen-printed carbon electrodes with a Nafion overlayer to stabilize the sensing interface and suppress ascorbic-acid interference (Hasan et al., 2023). This strategy illustrates how a polymer can improve analytical selectivity without acting as the principal electronic conductor. Nevertheless, the effect depends on analyte charge, coating amount, and measurement conditions; a membrane that excludes an interferent may also impede transport of a target or reaction product.

Structural polymers such as polycaprolactone (PCL) should be distinguished from conducting polymers. In the Ag@SiO_2–PCL fluorescence platform reported by Yun et al., electrospun PCL supplied a fibrous scaffold, while the silica-coated silver nanoparticles provided the metal-enhanced fluorescence functionality (Al-Gethami et al., 2022). The fibrous substrate supported greater protein loading than a conventional two-dimensional glass surface, and the silver-containing architecture produced higher fluorescence than the corresponding silica-coated PCL control. The improvement therefore arose from complementary structural and optical functions, rather than from PCL conductivity. Potential limitations include incomplete wetting, heterogeneous nanoparticle coverage, and restricted access to binding sites within the fibrous structure. Calcium alginate provides a hydrated, ionically crosslinked matrix for incorporating colloidal particles into a coherent sensing coating. Its selection can address particle retention and film formation, while

its carboxylate groups provide potential interaction sites for ionic analytes. Unlike a conducting polymer, however, alginate does not primarily establish electronic connectivity. In the $CoFe_2O_4$/Ca-alginate QCM system, its role is therefore associated with particle organization and the chemical and mechanical properties of the sensing layer. Polymer incorporation should not be assumed to improve performance under all conditions: the reported comparison with $CoFe_2O_4$-only coatings showed a temperature-dependent response. Moreover, swelling and coupled water can influence the acoustic signal, so frequency shifts should not be attributed exclusively to increased analyte binding. This example illustrates why polymer selection must be assessed against both its intended immobilization function and its effects on transduction (Carvalho et al., 2022).

Overall, polymer selection should be justified through an explicit relationship between the initial colloidal limitation, the proposed polymer function, and the resulting performance trade-off. Relevant comparisons include colloid-only and polymer-only interfaces, together with measurements of polymer loading or thickness, response time, signal retention, and component leaching where available. This approach distinguishes a demonstrated improvement in stability, selectivity, or accessibility from the unsupported assumption that adding a polymer necessarily enhances biosensor performance.

3.4 Interfacial thermodynamics, charge transfer, and mass transport

Interfacial engineering involves balancing nanoparticle retention and colloidal stabilization against the accessibility required for sensing. Electrostatic interactions, ligand binding, steric effects, and polymer–solvent compatibility influence particle association and attachment to a support. These interactions depend on the surrounding medium and cannot be inferred from particle composition alone. A dispersion that resists aggregation is also not necessarily thermodynamically stable; it may instead be kinetically stabilized by an interaction barrier. During immobilization and drying, changes in particle separation and ligand organization may alter the interface established in solution. Stability in dispersion and structural integrity after device fabrication should therefore be evaluated separately.

For electrochemical interfaces, increased current does not by itself demonstrate faster heterogeneous electron transfer. In a simple charge-transfer model, Butler–Volmer kinetics relates interfacial current to overpotential and exchange current density, whereas Marcus-type descriptions connect electron-transfer barriers with the driving force, reorganization energy, and electronic coupling. These frameworks provide interpretive models rather than evidence that every nanoparticle-modified interface follows the same mechanism. Carbonaceous supports can improve electrical connectivity, while ligand and polymer layers may introduce additional barriers depending on their thickness, electronic properties, and organization. Experimentally, DNA capping has been shown to alter silver nanoparticle oxidation, demonstrating that the surface coating can regulate electronic access to the nanoparticle core (Tanner et al., 2017; Hepburn et al., 2014).

Mass transport provides a separate constraint on hybrid-interface performance. Nanoparticle spacing determines whether local diffusion fields remain distinct or overlap, while an overlying film can change analyte partitioning and diffusion relative to the bulk solution. Consequently, an apparent increase in electrochemical response may arise without an increase in the intrinsic electron-transfer rate constant. Under a simplified one-dimensional diffusion model, the characteristic transport time scales as L^2/Deff, where L is the film thickness and Deff is the effective diffusion coefficient within the film. This relationship illustrates why additional polymer can improve immobilization while delaying analyte access. Mechanistic assessment should therefore combine electrochemical measurements with film thickness, nanoparticle coverage, and appropriate control interfaces rather than interpreting a larger current or lower fitted charge-transfer resistance as sufficient proof of interfacial synergy (Hepburn et al., 2014; Song et al., 2021).

4 Colloids in biosensors

Colloidal systems are essential in biosensor design, enhancing analytical performance in several ways. They can play a crucial role in signal amplification, where their composition and structure help amplify weak biological responses through mechanisms such as plasmonic enhancement in gold nanoparticles, fluorescence enhancement in semiconductor quantum dots, or electrochemical signal improvement in carbon-based nanomaterials. These effects collectively boost sensor sensitivity and reduce detection limits (Shukla et al., 2022). Colloids also serve as selective recognition platforms; their surfaces can be modified with biological elements such as enzymes, antibodies, aptamers, or nucleic acids to enable specific, high-affinity interactions with target analytes, such as small metabolites, pathogens, or protein biomarkers, thereby forming the foundation for accurate detection (Fu et al., 2024; Shukla et al., 2022). Additionally, colloids act as transducers, converting biochemical interactions into measurable physical signals, such as color changes, fluorescence variations, electrical current or impedance shifts, or changes in mass and vibration. By linking biological events to device readouts, colloids improve sensor communication (Fu et al., 2024; Shukla et al., 2022; Damborský et al., 2016; Yang et al., 2016). They also support stability and reproducibility, with well-designed colloidal surfaces maintaining structure and function in complex biological environments, reducing aggregation, background noise, and false signals. Their stability ensures reliable operation across multiple measurements, enhancing overall robustness (Fu et al., 2024; Shukla et al., 2022; Damborský et al., 2016; Geng et al., 2022; Yang et al., 2016).

4.1 Application areas of colloid biosensors

Colloidal biosensors are widely used in various fields, such as medical diagnostics, food safety, agriculture, point-of-care testing (POCT), and environmental monitoring, owing to their adjustable surface properties, high surface area, and strong signal amplification.

4.1.1 Medical diagnostics

In medical diagnostics, colloidal biosensors identify key biomolecules, including glucose, nitric oxide (NO), viral proteins,

hormones, antibodies, proteins, and extracellular vesicles (EVs). AuNPs, semiconductor quantum dots, and carbon-based fluorescent dots are used in optical and electrochemical sensing architectures (Yang et al., 2016). For example, fiber-optic surface plasmon resonance (FO-SPR) biosensors using colloids can detect breast cancer-related extracellular vesicles at levels around 10^7 particles/mL. Electrochemical colloidal sensors efficiently monitor glucose and NO levels, while piezoelectric and magnetic colloids aid in viral protein and antibody detection. Colloid-based biosensors support multiplexed, label-free detection, allowing rapid, noninvasive diagnostics suitable for POCT applications (Fu et al., 2024; Yang et al., 2016; Mondal et al., 2022).

4.1.2 Food safety and agriculture

Colloid-based biosensors are increasingly used in agriculture to enhance sustainability, reduce yield losses, and control environmental impacts (Yılmaz et al., 2022). They are effective for early warning, on-site analysis, and real-time monitoring, with high surface area and tunable optical and electrical properties for detecting low-concentration analytes. Commonly used for soil and water analysis, they detect nutrients like nitrate, nitrite, phosphate, ammonium, heavy metals, and pesticides (Rovira-Más et al., 2021). These sensors enable quick soil nutrient assessment, reducing unnecessary fertilizer use, costs, and pollution (Dyussembayev et al., 2021; Shaw and Honeychurch, 2022). Sensors with magnetic and gold nanoparticles provide accurate measurements even in complex soils (Rovira-Más et al., 2021). They also target plant health, detecting pathogens and stress markers early, such as proteins, enzymes, or VOCs linked to disease, thereby decreasing chemical pesticide use and crop loss (Chaturvedi et al., 2025). Additionally, they monitor post-harvest conditions by detecting gases such as ethylene and ammonia, helping to track ripening and spoilage. These cost-effective, portable sensors can be integrated into packaging or storage to extend shelf life and reduce food waste. In smart agriculture, colloid biosensors supply real-time data via wireless and IoT systems, optimizing irrigation, fertilization, and pest control. Overall, they promote controlled, eco-friendly, and efficient farming (Ali et al., 2020; He et al., 2025).

4.1.3 Point-of-care testing (POCT)

Colloid-based biosensors are vital for Point-of-Care Testing (POCT), enabling rapid, sensitive diagnostics outside labs. POCT delivers clinical results near patient care locations, such as clinics and homes. Colloidal nanomaterials offer properties such as portability, low cost, minimal sample preparation, rapid response, and high sensitivity. Widely used colloids include gold, silver, magnetic nanoparticles, quantum dots, and polymers (Nath and Ray, 2023; Wang et al., 2023). In conventional AuNP-based lateral-flow assays, the visible test line arises from the accumulation of nanoparticle-labelled recognition complexes at the capture region (Nath and Ray, 2023). Colloids are used in POCT to detect contagious diseases by functionalizing nanoparticles with recognition molecules, such as antibodies (Luppa et al., 2011). Their high surface area allows dense attachment of biorecognition elements, enabling sensitive detection at nanomolar or picomolar levels, which is essential for early diagnosis. Beyond infectious diseases, colloids are used in POCT for chronic and metabolic conditions, such as glucose sensors that improve electron transfer (Wang et al., 2023). They also aid in detecting cardiac, inflammatory, cancer biomarkers, and hormones from small samples like blood or saliva (Parihar et al., 2025). Magnetic nanoparticles provide sample preconcentration and purification, helping with complex fluids by binding targets and enabling magnetic separation, enhancing specificity and reproducibility (Nath and Ray, 2023). Colloids facilitate integration into miniaturized platforms like paper-based devices, microfluidics, and wearables. Paper biosensors are inexpensive, disposable, and easy to use, especially when paired with smartphone readouts for quantification and health tracking. Challenges include stability over time, reproducibility, and mass production. Stability under varying conditions and regulatory hurdles need addressing. Advances in surface chemistry, bioconjugation, and biodegradable materials are improving system robustness. Overall, colloid biosensors are key for modern POCT, combining sensitivity, speed, and user-friendliness to support decentralized, personalized healthcare, especially in resource-limited settings (Huang et al., 2023).

4.1.4 Environmental monitoring

Colloid-based biosensors are increasingly used for environmental monitoring, enabling rapid, sensitive, on-site detection of contaminants in water, soil, and air. They are sensitive, selective, portable, robust, and capable of real-time measurements due to their high surface area and unique properties (Koedrith et al., 2015). In water quality monitoring, colloid-based biosensors detect heavy metals, organic pollutants, and pathogens (Hemdan et al., 2024). Gold and silver nanoparticles are used for colorimetric sensing of metals such as mercury and arsenic, relying on aggregation or plasmon shifts (Nath and Ray, 2023). Enzyme- and aptamer-functionalized nanoparticles detect pesticides and endocrine disruptors. In soil, colloidal sensors detect pesticides, hydrocarbons, and heavy metals, aiding sustainable land management by providing rapid feedback on contamination (Yılmaz et al., 2022; Chaturvedi et al., 2025). In the air, sensors detect volatile organic compounds, gases, and pathogens, with nanoparticle-based chemiresistive and optical sensors seeing use in urban and industrial monitoring. Increasingly, colloid biosensors are integrated into autonomous systems with microfluidics and wireless data transmission, enabling remote monitoring, early spill warnings, and pollution tracking. Challenges include sensor fouling, interference, stability, and calibration issues, prompting ongoing research on functionalization, antifouling coatings, and eco-friendly materials (Xu et al., 2010). Figure 4 shows the map of colloidal materials and their roles in biosensing.

5 Carbon- and polymer-integrated colloidal platforms in biosensing

The following sections evaluate colloidal sensing platforms according to the contribution of their carbonaceous and polymeric components. Particular attention is given to whether

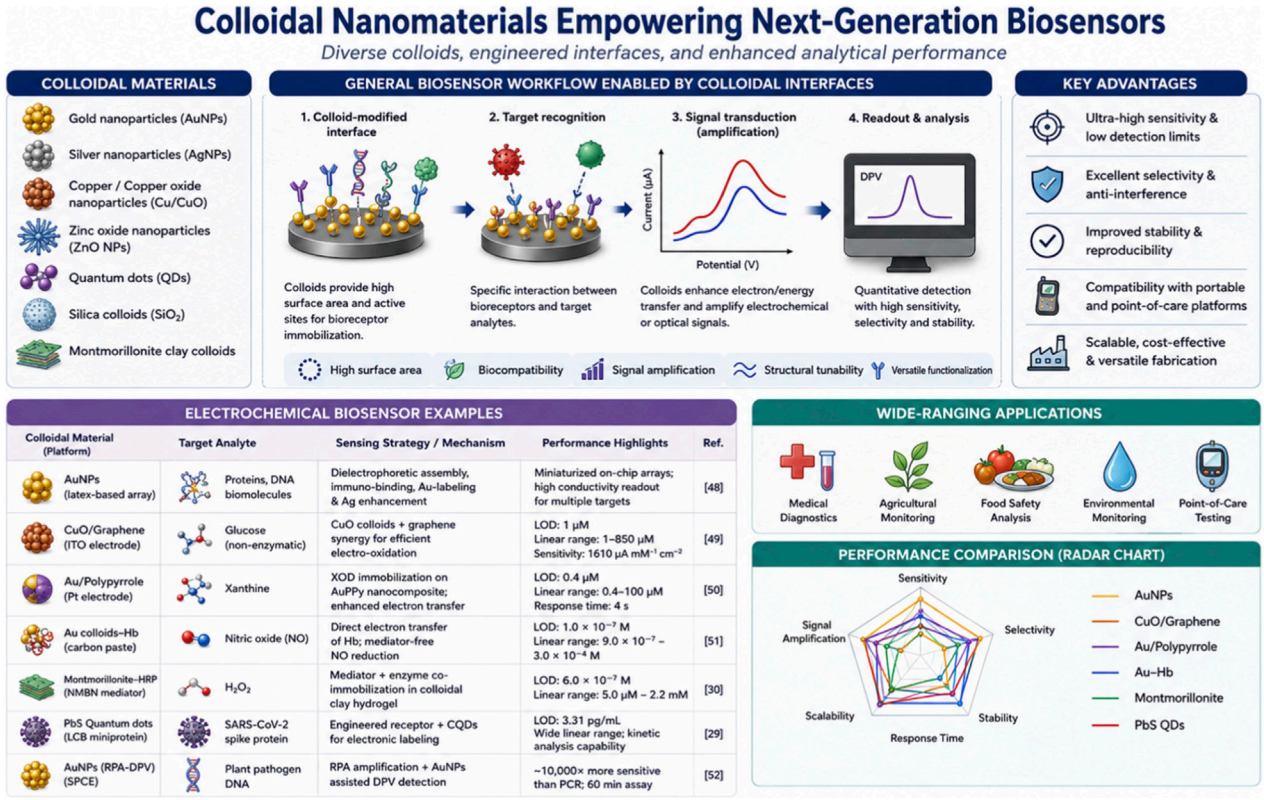


FIGURE 4
Functional map of colloidal materials and their roles in biosensing.

hybridization improves performance relative to the corresponding unmodified electrode, colloid-only interface, or carbon/polymer support. Where such controls are unavailable, the reported analytical performance is distinguished from evidence of a specific hybridization benefit. Comparisons prioritize studies targeting the same analyte under comparable measurement conditions, because differences in detection limit alone do not establish the superiority of one material architecture over another.

5.1 Electrochemical biosensors

Electrochemical colloidal platforms can be fabricated by preparing particles before electrode modification or by generating them directly on the sensing surface. These routes produce different particle–support contacts and must be distinguished when interpreting analytical performance. Carbonaceous supports provide the electrode framework or conductive pathways, while polymeric matrices can retain particles and bioreceptors. AuNPs additionally offer electrochemical functionality and compatibility with thiol-based surface modification, although their contribution depends on loading, surface ligands, and integration with the electrode (Huang et al., 2023).

For an *ex situ* carbon-supported configuration, Xu et al. used preformed gold colloids to modify a carbon paste electrode and subsequently immobilized hemoglobin by adsorption. The resulting protein–AuNP–carbon interface supported mediator-free electrocatalytic reduction of nitric oxide, with a reported detection limit of 1.0×10^{-7} M. Carbon paste supplied the conductive support, while the colloidal gold-containing surface provided the interface for protein immobilization. This configuration illustrates a relatively direct assembly strategy, but the analytical response must be interpreted in relation to the accessible protein population and the distribution of gold within the exposed paste surface (Lau et al., 2017).

Lau et al. employed a more explicitly separated synthesis-and-transfer workflow. AuNPs were prepared by citrate reduction of $HAuCl_4$ and functionalized with DNA probes before recognition of RPA-amplified pathogen sequences. Streptavidin-coated magnetic beads enabled capture and washing of the labeled complexes; following thermal treatment, the resulting solution was transferred to a screen-printed carbon electrode and air-dried. Electrochemical oxidation of gold followed by DPV reduction provided the analytical readout. Here, the carbon electrode served as the receiving transducer, whereas AuNPs functioned as labels rather than as a permanent catalytic coating. The complete assay was approximately 10,000-fold more sensitive than conventional PCR/gel electrophoresis. This improvement belongs to the combined amplification, capture, and readout workflow and cannot be attributed exclusively to nanoparticle-induced electron transfer (Devi et al., 2012).

Carbon–metal oxide integration provides a different architecture. Mubarakali et al. (Devi et al., 2012) incorporated flower-shaped CuO nanoparticles into a graphene-modified indium tin oxide (ITO) electrode for non-enzymatic glucose detection (Figure 5). CuO

supplied catalytic sites, while graphene could contribute to electrical connectivity and particle distribution. The reported detection limit was 1 μM, with a sensitivity of 1610 μA mM^{-1} cm^{-2}. These results establish the analytical performance of the assembled interface; they do not independently demonstrate that graphene protects CuO from chemical transformation. Assessment of this proposed benefit requires matched stability measurements and characterization before and after operation (Devi et al., 2012).

Devi et al. prepared Au–polypyrrole (AuPPy) colloids by oxidizing pyrrole with $HAuCl_4$ in a cetyltrimethylammonium bromide solution. The preformed composite was cast onto a platinum electrode, followed by xanthine oxidase immobilization using glutaraldehyde. This route combined nanoparticle formation and polymer synthesis before transferring the composite to the transducer. The Au-containing phase and PPy matrix together provided the enzyme-bearing electrochemical interface. The sensor exhibited a detection limit of 0.4 μM, a linear range of 0.4–100 μM, and a response time of 4 s. Approximately 40% activity loss was reported after 200 uses over 100 days with storage at 4 °C. This result provides a practical durability measure, although it does not distinguish enzyme deactivation from other changes in the composite interface (Wu et al., 2018).

In contrast, Wu et al. constructed a ternary interface using electrodeposition and sequential enzyme assembly. A PPy–RGO film was first formed on a glassy carbon electrode, after which AuNP electrodeposition and glucose oxidase assembly were alternated to produce multilayers. This is an *in situ* particle-growth reference rather than deposition of preformed colloidal AuNPs. The architecture combined a carbonaceous framework, conducting polymer, and nanoparticle/enzyme layers, yielding a glucose detection limit of 5.6 μM and a linear range of 0.2–8 mM. The fabrication sequence illustrates control over interfacial organization, while increasing the number of layers introduces a balance between enzyme loading and access to the underlying electrochemical interface (Lei et al., 1996).

Additional platforms provide useful comparisons with carbon/polymer hybrids. Lei et al. co-immobilized New Methylene Blue N and horseradish peroxidase in a sodium montmorillonite hydrogel for H_2O_2 detection, obtaining a linear range of 5.0 μM–2.2 mM. The clay matrix supplied adsorption and confinement sites for organizing the enzyme–mediator interface (Zhao et al., 2024). Zhao et al. instead combined PbS colloidal quantum-dot labels with the LCB miniprotein receptor and obtained a detection limit of 9.58 fg mL^{-1} using a high-electron-mobility transistor

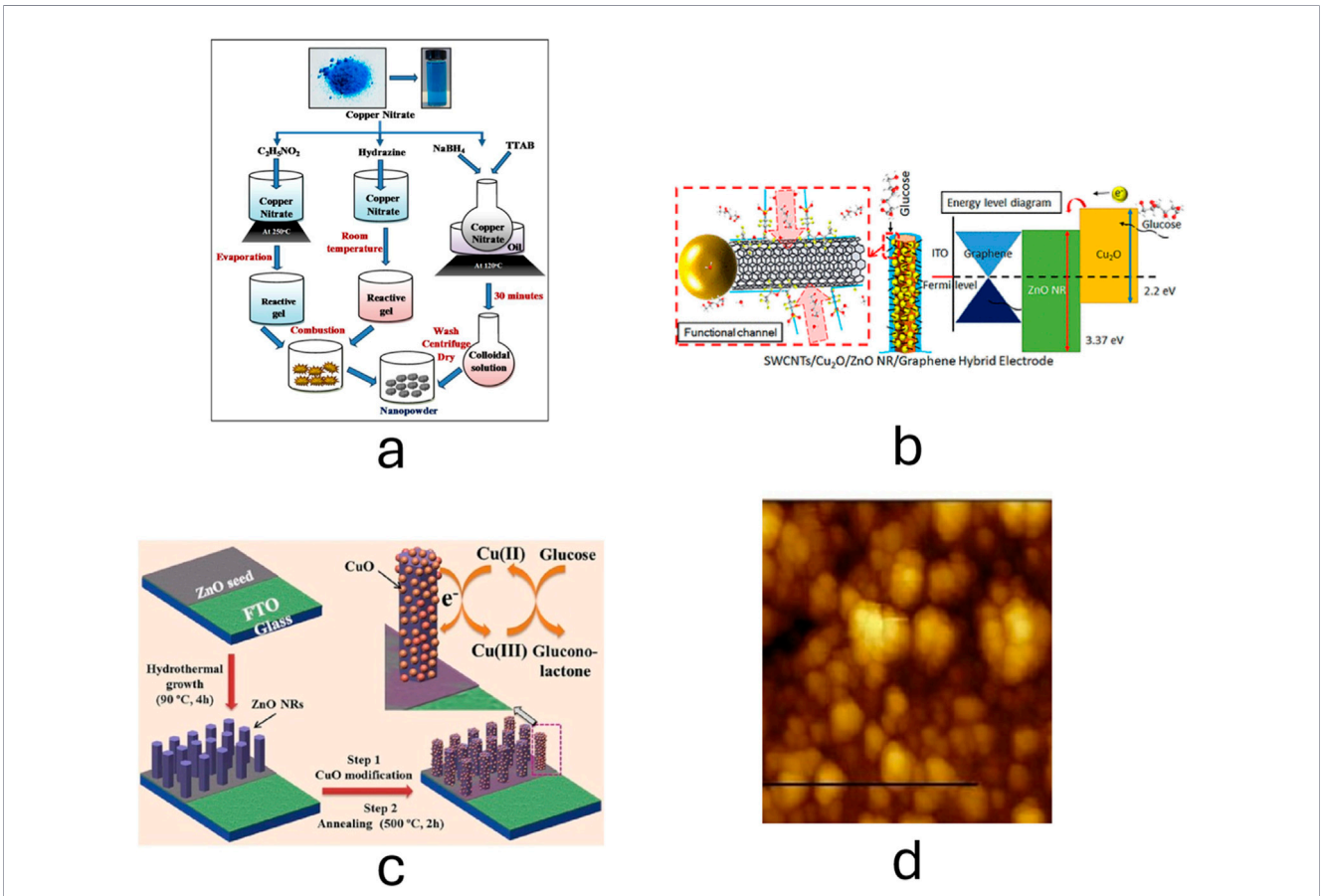


FIGURE 5
Four panels show copper-based nanomaterial synthesis and glucose-sensing interfaces. (**a**) is a flowchart with three routes from copper nitrate to nanopowder. It shows reagent addition, heating, and processing steps. (**b**) shows a hybrid electrode made of single-walled carbon nanotubes, Cu_2O, ZnO nanorods, and graphene, alongside an energy-level diagram (Chen et al., 2020). (**c**) shows ZnO nanorods grown on fluorine-doped tin oxide glass, followed by CuO coating and annealing. An inset illustrates electron transfer during glucose oxidation. Figure 1 from Ahmad et al. (2017). (**d**) shows a granular surface with rounded bright features separated by darker regions.

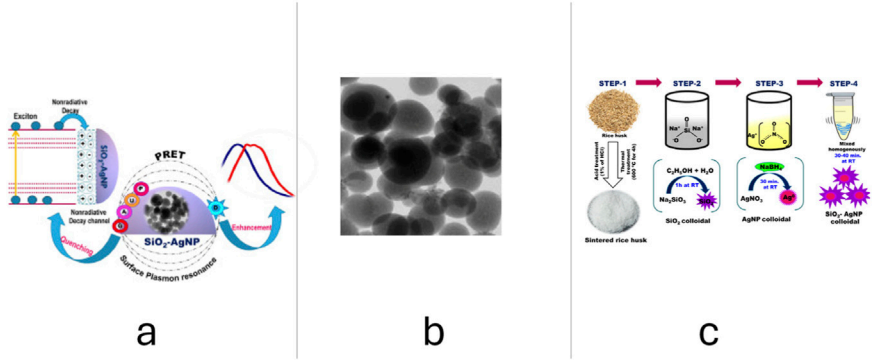


FIGURE 6
Silica–silver (SiO_2–Ag) colloidal nanoparticles for fluorescence-based biosensing. (**a**) Schematic of plasmon resonance energy transfer (PRET) and the associated fluorescence response. (**b**) Transmission electron micrograph of the colloidal nanoparticles. (**c**) Synthesis of SiO_2–Ag colloidal nanoparticles using rice husk as the silica precursor (Soundharraj et al., 2021).

(HEMT) readout (Animashaun et al., 2025). These examples represent alternative immobilization and labeling strategies rather than direct evidence of carbon/polymer-assisted enhancement. Across all configurations, comparisons should consider fabrication, analyte, sample matrix, and validation conditions alongside the detection limit.

Recent studies extend carbon–polymer–nanoparticle integration toward selective and wearable sensing. A 2025 lactate sensor combined laser-induced graphene, AuNPs, and a PEDOT-based molecularly imprinted polymer, integrating a carbon electrode framework with a nanoparticle-containing recognition layer (Chen et al., 2026). A 2026 wearable glucose sensor employed P (EDOT-MeOH), carboxylated multiwalled carbon nanotubes, and AuNPs, illustrating the incorporation of a conducting polymer–carbon–metal architecture into a flexible device (Mubarakali et al., 2023). These examples motivate evaluation of recognition selectivity and electrical performance alongside coating adhesion and response under deformation. MXenes provide a complementary conductive support rather than an interchangeable substitute for graphene. A 2025 MXene/AuNP wearable cortisol aptasensor reported LODs of 0.10 ng mL^{-1} in PBS and 0.14 ng mL^{-1} in artificial sweat over a 0.5–500 ng mL^{-1} detection range. This matrix-dependent difference illustrates why buffer performance should be distinguished from performance in the intended sampling medium.

5.2 Optical biosensors

Optical colloidal platforms differ according to whether particles remain dispersed, are incorporated into a polymeric scaffold, or are grown directly on a substrate. Their preparation and integration determine particle spacing, receptor accessibility, and the optical interactions responsible for detection. Polymer scaffolds can provide a receptor-bearing structure, carbon components can act as fluorescent reporters, and inorganic coatings can regulate surface functionalization or fluorophore–metal separation. These functions must be distinguished rather than assigning all improvements to increased surface area.

Soundharraj et al. (2021) prepared silica colloids by a sol–gel route using rice husk-derived material as the precursor and subsequently combined them with silver colloids. The resulting SiO_2–Ag dispersion was used for fluorescence-based biomolecular sensing through a reported plasmon resonance energy transfer mechanism, achieving a glucose detection limit of 0.49 μM (Figure 6). This is a solution-phase inorganic reference rather than a carbon- or polymer-supported surface coating. Its practical assessment should therefore include dispersion stability and matrix-dependent changes in fluorescence, rather than electrode adhesion or film conductivity (Zhao et al., 2008).

Yun et al. demonstrated a polymer-supported optical interface through a sequential electrospinning, photoreduction, and silica-coating process. Electrospun PCL fibers provided the scaffold, silver nanoparticles were formed on the fibers, and silica coating produced the Ag@SiO_2–PCL architecture. PCL supplied the three-dimensional protein-loading structure, Ag provided plasmonic enhancement, and silica regulated separation between the metallic surface and fluorescent assay components. The fibrous substrate supported greater protein loading than conventional glass, while the silver-containing structure produced higher fluorescence than silica-coated PCL without Ag. These comparisons support complementary structural and optical contributions. Reproducible performance nevertheless requires control of particle coverage and coating geometry; the improvement should not be attributed to PCL conductivity (Al-Gethami et al., 2022).

Dispersed AuNP assays illustrate an alternative in which surface functionalization replaces permanent immobilization. Zhao et al. attached DNA aptamers to preformed AuNPs and investigated their resistance to salt-induced aggregation. Folded aptamer structures stabilized the colloids more effectively than the corresponding unfolded structures under the investigated conditions. The functional DNA layer therefore participated in both molecular recognition and regulation of the colloidal optical response. This mechanism depends on aptamer organization and solution conditions, requiring control of ionic strength and surface coverage during assay preparation (Wang et al., 2018).

Carbon-containing optical assays can instead couple colloids with a fluorescent reporter. An acetamiprid aptasensor combined preformed AuNPs, fluorescent carbon dots, and an aptamer-based recognition scheme, using the inner filter effect to modulate fluorescence. The carbon dots supplied the emissive signal, while AuNP absorption regulated the measured intensity. Unlike a conductive carbon-supported electrode, this system operated through interactions between dispersed optical components. Its interpretation therefore requires distinction between absorption-mediated attenuation and other quenching mechanisms, together with evaluation of aggregation and sample background (Huang et al., 2020).

For lateral-flow integration, Zhang et al. conjugated anti-human IgM to colloidal AuNP reporters and incorporated them into an immunochromatographic strip. SARS-CoV-2 nucleoprotein immobilized at the test line captured the target antibody-containing complexes, producing a visible signal. The particles supplied the optical label, while the porous membrane provided capillary transport and spatial separation of capture and control regions. The reported diagnostic sensitivity and specificity were 100% and 93.3%, respectively. These values characterize the evaluated clinical sample set rather than analytical sensitivity, and broader applicability requires independent validation and assessment of conjugate stability (Mirshe et al., 2024).

Mirshekari et al. prepared silica-coated gold nanorods and functionalized the coating for covalent attachment of anti-Müllerian hormone antibodies. This sequence produced a receptor-bearing LSPR interface in which target recognition was monitored through changes in peak position. The metallic component supplied the plasmonic response, while functionalized silica enabled construction of the recognition layer. Comparison with ELISA supported evaluation against an established assay, although this does not independently establish equivalent diagnostic performance across populations. Nonspecific adsorption and matrix-dependent refractive-index changes remain important validation considerations (Wang et al., 2026).

Conductive hydrogels also extend hybrid integration to electrochemiluminescent sensing. A 2026 study by wang et al. constructed a MXene/Au–Ag nanocluster/bovine serum albumin (BSA) hydrogel through a one-pot route, combining a conductive nanosheet network with a protein-based matrix and luminescent nanoclusters. The platform reported a glutathione LOD of 340 pM (Zhao et al., 2026). Its relevance lies in the distinct structural, transport, and reporting functions of the constituents; durability and antifouling claims should be evaluated using their corresponding experimental controls. In AI-assisted optical analysis, a 2026 study combined an Ag@Pt/porous-silicon Bragg-mirror substrate with deep learning for celecoxib detection in serum (Kim et al., 2023). This provides a recent analytical reference, while its applicability to other substrates or sample populations requires separate validation. The associated dataset and model-validation requirements are discussed in Section 6.

Finally, Kim et al. constructed the ZnO–Au SERS-based direct amplification platform by depositing gold on oriented ZnO nanorods. This directly fabricated inorganic substrate is retained as an *in situ* reference rather than an *ex situ* colloidal coating. ZnO organized the metallic architecture, while Au-containing regions provided Raman enhancement. The deep-learning-assisted ZADA system reported a diagnostic sensitivity of 100% in the evaluated dataset, with an assay time of less than 20 min (Soundharraj et al., 2021). This result should be interpreted within the study's validation design and does not establish equivalent performance across independent patient cohorts, substrate batches, or measurement settings.

Together, these examples connect preparation and integration with distinct optical functions: scaffold-supported loading, dispersion-dependent aggregation, fluorescence modulation, membrane-based reporting, and immobilized plasmonic detection. Stability and reproducibility should be assessed using measurements appropriate to each configuration rather than inferred from initial signal enhancement alone (Table 3).

5.3 Piezoelectric and magnetic biosensors

Colloidal materials contribute to acoustic and magnetic biosensors through different mechanisms. In quartz crystal microbalance (QCM) systems, nanoparticle-containing coatings modify the receptor-bearing interface and its acoustic response. In magnetoresistive (MR) devices and magnetic lateral-flow assays, magnetic particles primarily serve as detectable labels and, where implemented, as tools for sample manipulation. Carbonaceous coatings and polymeric matrices can provide additional functionalization or immobilization capabilities, but their benefits depend on how they affect target accessibility, particle organization, and signal reproducibility. These architectures should therefore be compared according to their integration method and transduction mechanism rather than treated as equivalent forms of mass amplification.

Reyes et al. fabricated a ZnO-modified QCM by growing vertically aligned nanotips directly on the sensing surface using metalorganic chemical vapor deposition (MOCVD). The ZnO architecture provided a nanostructured surface for subsequent DNA functionalization, while its superhydrophilic state supported sample spreading. The modified device exhibited a more-than-tenfold increase in mass-loading sensitivity compared with a conventional QCM, and selective DNA immobilization and hybridization were demonstrated. However, these nanotips were grown directly on the substrate rather than deposited from a preformed colloidal dispersion. This system is therefore included as an *in situ* nanostructuring reference, with potential fabrication constraints associated with the growth process and control of surface morphology (Al-Gethami et al., 2022).

Polymer-containing coatings offer a different integration strategy. Al-Gethami et al. incorporated green-synthesized $CoFe_2O_4$ nanoparticles into calcium alginate and deposited the resulting nanocomposite on QCM sensors for Pb(II) detection. The ferrite supplied the inorganic particulate component, while the alginate introduced a polymeric matrix with functional groups capable of participating in ion association. Comparisons with $CoFe_2O_4$-only coatings showed that the effect of polymer incorporation depended on temperature. At 25 °C, the reported frequency shifts were 27.49 ± 0.81 Hz for $CoFe_2O_4$ and 25.85 ± 0.85 Hz for the composite; at 35 °C, the corresponding values were 23.63 ± 0.90 and 33.87 ± 0.73 Hz. These results do not support a universal enhancement following alginate incorporation.

TABLE 3 Colloidal materials in optical, piezoelectric, and magnetic sensing platforms.

Biosensors	Colloidal material	Target analyte	Sensor principle/ architecture	Key findings & performance	References
Optical	Gold nanoparticles (AuNPs) + folded/ unfolded DNA aptamers	Adenosine, K^+, ADA-related inhibitors	Aptamer folding controls AuNP stabilization; aggregation-based colorimetric sensing	Folded aptamers provide superior steric/electrostatic stabilization, enabling tunable aggregation–redispersion, and are used for colorimetric detection of small molecules	Ben Haddada et al. (2018)
	SiO_2 and SiO_2 –Ag colloidal nanoparticles	Glucose, uric acid, paracetamol, ascorbic acid, dopamine	Fluorescence-based sensing via plasmon resonance energy transfer (PRET)	Strong fluorescence at 325 nm; glucose LOD 0.49 μM; ~99% recovery in urine and serum; validated for multi-biomolecule detection	Mirshe et al. (2024)
	Silica-coated gold nanorods (SiO_2@ Au-NRs)	Anti-Müllerian hormone (AMH)	LSPR biosensor with covalently attached antibodies	LOD 0.086 ng/mL, LOQ 0.262 ng/mL; ELISA-comparable accuracy; reduced cost and time; high LSPR redshift sensitivity	Yun et al. (2019)
	Silver-decorated PCL fibers with silica shell (Ag@SiO_2-PCL)	IgG (immunobinding)	Metal-enhanced fluorescence (MEF) on electrospun fibers	Substantial fluorescence enhancement controlled by silica thickness; higher protein-loading; superior sensitivity vs. glass slides and SiO_2 -PCL	Pan et al. (2024)
	Self-assembled photoreactive colloidal nanoparticles (AuNP-based)	DNA, proteins, exosomes (multiplex)	Nanophotonic biosensor using colloidal superstructures	Label-free detection; simultaneous multi-target sensing; affordable, rapid, and suitable for point-of-care use	Wu et al. (2025)
	Colloidal gold nanoparticles (AuNP-LF test strips)	SARS-CoV-2 IgM antibodies	Lateral-flow immunoassay using AuNP-IgM conjugates	100% sensitivity, 93.3% specificity; 15-min results; cross-reactivity was evaluated against the tested viral panel	Jhuang et al. (2021)
	ZnO-Au nanorod SERS substrate	Viral nucleic acids (COVID-19 samples)	Direct on-chip amplification + SERS + deep learning (ZADA system)	92.31% sensitivity, 81.25% specificity; deep learning raises sensitivity to 100%; rapid label-free detection in 20 min	Reyes et al. (2009)
Piezoelectric	ZnO colloidal nanotips grown on QCM surface	DNA oligonucleotides	Piezoelectric nano-QCM with ZnO nanotip arrays; superhydrophilic surface enhances mass loading	>10× higher mass sensitivity vs. standard QCM; selective DNA immobilization and hybridization confirmed via fluorescence; dense, vertically aligned ZnO nanotips improve performance	Al-Gethami et al. (2022)
	$CoFe_2O_4$ NPs and $CoFe_2O_4$/Ca-alginate nanocomposite	Pb(II) ions	QCM nanosensor using magnetic–biopolymer composite coating	Temperature-dependent coating response: At 25 °C, frequency shifts were 27.49 Hz for $CoFe_2O_4$ and 25.85 Hz for the composite; at 35 °C, the corresponding values were 23.63 and 33.87 Hz. This is a chemical ion-sensing References	Moyano et al. (2020)

(*Continued*)

TABLE 3 Continued

Biosensors	Colloidal material	Target analyte	Sensor principle/ architecture	Key findings & performance	References
	AuNP-coated quartz via SAM-assisted nanostructuring	Staphylococcal enterotoxin A (SEA)	Piezoelectric immunosensor (QCM-D) with AuNP-nanostructured surface	Larger frequency shifts; LOD 8 ng/mL (vs. 20 ng/mL flat chips); sandwich assay LOD ≈1 ng/mL; improved antigen access drives superior sensitivity; ~25 min test time	Malathi et al. (2022)
	Fe_3O_4@C nanoflowers	Extracellular vesicles; biotin-binding assays	Magnetic lateral-flow immunoassay	Strong magnetic response; LOD better than prior MNP labels within 0–3 × 10^7 EVs/μL; highly reproducible (RSD ~3%); effective quantification in plasma samples	Campanile et al. (2022)
	Core@satellite magnetic particles	Human IgG	Magnetoresistive biosensor	LOD 13 pM (2 ng/mL); stable magnetic properties; direct antibody immobilization; portable and multiplex-capable platform suitable for point-of-care diagnostics	Zhao et al. (2008)

Moreover, this is a chemical ion-sensing example rather than a bioreceptor-based biosensor. It provides a useful reference for polymer–particle interface design, but frequency shifts alone cannot establish improved detection limits or distinguish ion uptake from changes in coating hydration and mechanical properties (Moyano et al., 2020).

Ben Haddada et al. examined preformed AuNPs immobilized on gold- or silicon-coated quartz surfaces using thiol- and amine-terminated self-assembled monolayers (Malathi et al., 2022). Anti-staphylococcal enterotoxin A (SEA) antibodies were subsequently attached, and antigen binding was monitored by QCM with dissipation monitoring (QCM-D). The AuNPs provided a curved receptor-bearing interface, while the molecular linkers anchored them to the substrate. Compared with planar controls, the nanostructured sensors exhibited larger antigen-binding responses despite similar antibody coupling densities. The direct-assay detection limit decreased from 20 to 8 ng mL^{-1}, while a sandwich configuration achieved approximately 1 ng mL^{-1} within 25 min. These observations support improved accessibility of antigen-binding sites as a possible explanation, rather than proving a specific antibody orientation. Interpretation also requires consideration of dissipation and coupled solvent, because the acoustic response of a hydrated interface is not determined solely by the dry mass of captured antigen.

Carbon-coated magnetic particles illustrate a more direct contribution of carbon–colloid integration. Moyano et al. prepared superparamagnetic Fe_3O_4@C nanoflowers using a one-pot solvothermal route. The multicore iron oxide structure supplied the magnetic response, while the carbon coating provided optical contrast and a functionalizable outer surface (Campanile et al., 2022). The particles were evaluated as labels in lateral-flow immunoassays, including a biotin–neutravidin model and extracellular-vesicle (EV) detection. The study reported an RSD of approximately 3%, an EV working range of 0–3 × 10^7 EV μL^{-1}, and application to plasma samples. The reported EV detection limit was lower than previously described values for other magnetic labels, although comparisons between studies do not isolate the contribution of the carbon coating. Establishing that contribution requires matched particles with and without carbon, together with evaluation of conjugation efficiency, membrane transport, and nonspecific retention.

Campanile et al. constructed an inorganic core@satellite architecture by attaching AuNPs to commercial iron oxide clusters. Photochemical immobilization was then used to attach antibodies to the gold satellites, combining a receptor-functionalization surface with a magnetic core (Chaturvedi et al., 2025). On an MR biochip, these particles enabled human IgG detection in water with a detection limit of 13 pM, equivalent to approximately 2 ng mL^{-1}. This result demonstrates compatibility between the particle architecture, antibody attachment, and magnetic readout. However, validation in water does not establish performance in serum or other complex matrices, and the architecture alone does not guarantee long-term colloidal stability. It is therefore retained as a reference for separating magnetic and bioconjugation functions, rather than as direct evidence of carbon- or polymer-assisted enhancement.

Together, these examples distinguish polymer-mediated coating formation, carbon-coated magnetic labeling, and inorganic surface nanostructuring. Their analytical performance reflects different combinations of target recognition, interfacial accessibility, acoustic coupling, and magnetic detection. Comparisons should therefore consider sample matrix, assay format, component-specific controls, stability, and fabrication reproducibility alongside the reported detection limits (Table 4).

The comprehensive evaluation presented in this comparative matrix clarifies that the architectural success of next-generation biosensing interfaces depends on matching the specific physical

TABLE 4 Cross-transduction modality matrix: Advantages, limitations, and sensing profiles of core colloidal platforms.

Colloidal material	Electrochemical biosensors	Optical biosensors	Piezoelectric/ magnetic biosensors	Main advantages	Main limitations	Refs.
Gold nanoparticles (AuNPs)	Excellent electron transfer and conductivity	Strong SPR/LSPR activity	Enhanced antigen accessibility on QCM surfaces	Easy functionalization, high sensitivity	Aggregation, high cost	Lau et al. (2017), Xu et al. (2010), Huang et al. (2020), Ben Haddada et al. (2018), Soundharraj et al. (2021)
Silver nanoparticles (AgNPs)	Not assessed in the cited optical examples	Strong SERS and MEF enhancement	Limited	High plasmonic enhancement	Oxidation instability	Al-Gethami et al. (2022), Patra and Mishra (2026)
PbS quantum dots	CQD electrochemical labeling	Fluorescence and optical amplification	Limited	Ultra-low detection limit	Potential toxicity	Animashaun et al. (2025)
ZnO nanostructures	High electrochemical activity	SERS enhancement	Strong QCM enhancement	Large surface area, rapid kinetics	Surface degradation	Soundharraj et al. (2021)
Clay colloids (montmorillonite)	Excellent mediator stabilization	Not evaluated in the cited study	Not evaluated in the cited study	High adsorption and ion exchange	Lower conductivity	Campanile et al. (2022)
Magnetic nanoparticles (Fe_3O_4, $CoFe_2O_4$)	Sample enrichment	Limited	Excellent magnetic manipulation	Efficient separation and concentration	Agglomeration risk	Moyano et al. (2020), German et al. (2022)

TABLE 5 Detection limits and linear ranges of the electrochemical sensing platforms included in Figure 5.

Target analyte	Sensing platform	LOD (μM)	Linear range (μM)	References
Glucose	CuO–graphene/ITO	1	1–850	Xu et al. (2010)
Glucose	PPy–rGO–$(AuNPs–GOD)_4$/glassy carbon	5.6	200–8000	Hepburn et al. (2014)
Xanthine	Xanthine oxidase/Au–PPy/Pt	0.4	0.4–100	Yun et al. (2019)
Nitric oxide	Hemoglobin/Au colloids/carbon paste	0.1	0.9–300	Lau et al. (2017)
Hydrogen peroxide	Montmorillonite–HRP–New methylene blue N/glassy carbon	0.6	5–2200	Zhao et al. (2024)

properties of a colloidal material with the requirements of the transduction platform. Instead of looking at these nanomaterials in isolation, this matrix highlights how a single colloidal core can be multi-functional, showing distinct operational profiles across electrochemical, optical, and mechanical detection pathways (Table 5). Noble metal colloids, particularly gold nanoparticles (AuNPs), serve as a reliable baseline due to their high electronic conductivity and plasmonic properties. As indicated in the matrix, AuNPs provide distinct advantages across all three modalities: they accelerate direct electron transfer in electrochemical systems, drive colorimetric shifts in optical assays, and reduce steric hindrance on acoustic surfaces like Quartz Crystal Microbalances (QCM) to improve antigen accessibility. However, their widespread industrial application remains limited by high raw material costs and an inherent tendency toward salt-induced aggregation. Silver nanoparticles (AgNPs) offer even stronger plasmonic field enhancements for surface-enhanced Raman scattering (SERS) and Metal-Enhanced Fluorescence (MEF), but they face critical trade-offs regarding oxidation and long-term chemical instability.

Transition metal oxides and semiconductor nanocrystals offer alternative design choices. Zinc oxide (ZnO) nanostructures provide versatile morphological options (such as vertically oriented nanotips or nanorods) that modify surface morphology and the accessible sensing interface and more than tenfold improvements in QCM mass-loading performance. Similarly, lead sulfide (PbS) colloidal quantum dots (CQDs) utilize quantum confinement to support electronic labeling strategies, yielding ultra-low, femtomolar-level detection limits on specialized chip substrates. Nevertheless, both systems face limitations: ZnO is prone to surface degradation in aqueous solutions, while cadmium- or lead-based quantum dots raise long-term toxicity concerns. Finally, the matrix highlights the roles of clay colloids (such as montmorillonite) and magnetic nanoparticles (Fe_3O_4 and $CoFe_2O_4$). These materials are typically integrated into hybrid setups to address the limitations of single-component systems. Montmorillonite clay exhibits relatively low standalone electrical conductivity, but its layered silicate sheets provide excellent ion-exchange capacities and structural support

to immobilize sensitive enzymes and retain redox mediators within the sensing matrix and limit mediator leaching. Concurrently, magnetic nanostructures introduce excellent magnetic manipulation features. This enables rapid sample enrichment, preconcentration, and automated target separation directly from complex, non-pretreated biological fluids like human plasma. In summary, this comparative analysis shows that future biosensor designs should move away from single-material components. Instead, the field is transitioning toward engineered hybrid colloids—such as silica-encapsulated metallic cores or polymer-shielded transition metal oxides—to optimize signal amplification while overcoming instability and chemical degradation.

5.4 Critical comparison of hybrid interfaces and analytical performance

The reported performance of colloidal hybrid biosensors depends on material composition, interfacial organization, and assay conditions. Carbon incorporation can improve electrical connectivity or nanoparticle distribution, but its contribution must be distinguished from changes in accessible area, catalyst loading, and receptor coverage. Accordingly, comparisons between graphene-, polymer-, and colloid-containing interfaces are most informative when the same analyte and measurement protocol are used with appropriate component-omission controls. Differences between unrelated sensors do not independently establish a material-specific advantage.

Polymer selection introduces a balance between component retention and analyte accessibility. In a comparative study of glucose biosensors based on dendritic gold-modified graphite electrodes, PPy produced 1.35-fold higher sensitivity and a 2.57-fold lower detection limit than PANI under the investigated conditions (Devi et al., 2012). This within-study comparison supports an effect of polymer selection, but it does not establish universal superiority of PPy. Polymer thickness, doping, porosity, and nanoparticle distribution must also be considered. Where thickness or nanoparticle/polymer ratio was not measured, an optimum deposition time or precursor concentration should not be interpreted as a quantitatively established structural optimum.

Surface charge provides another condition-dependent variable. It can influence colloidal dispersion, receptor association, and nonspecific interactions, but zeta potential measured in a synthesis medium does not establish stability in serum or the final assay buffer. Comparisons should therefore specify the measurement medium, pH, and available aggregation measurements. After immobilization, dispersion measurements should be complemented by assessment of coating integrity and particle retention.

Durability must likewise be evaluated using the reported test protocol. Devi et al. reported approximately 40% activity loss after 200 uses over 100 days with storage at 4 °C, corresponding to approximately 60% retained activity (Wu et al., 2018). This combined use-and-storage result should not be described as either pure shelf-life stability or 200 regeneration cycles. More generally, signal retention should be reported with its time point, storage conditions, and measurement history. Values at approximately 1 week, 1 month, or 3 months can be compared where available, but unreported time points should not be interpolated without a justified model.

Analytical detection limits require similar qualification. Unit conversion enables comparison only for the same analyte and does not remove differences in sample preparation, assay format, or calculation method. Electrochemical calibration slopes expressed per unit electrode area cannot be directly compared with unnormalized currents, optical intensity changes, or diagnostic classification sensitivity. Furthermore, a low detection limit has practical value only when considered alongside the relevant concentration range, quantification capability, matrix effects, and sample dilution. For example, detection of abundant metabolites may depend more on an appropriate working range and interference control than on the lowest achievable LOD (Devi et al., 2012; Wu et al., 2018).

Finally, real-sample validation and fabrication consistency determine whether an analytical improvement is transferable beyond laboratory conditions. Recovery from spiked samples, measurement of endogenous analytes, and agreement with a reference method provide different levels of evidence and should be identified separately. Likewise, simple fabrication or a disposable format does not establish scalability without device-to-device or batch-to-batch data. The revised comparisons therefore distinguish demonstrated performance from proposed advantages and identify missing structural, stability, and validation information as limitations of the available evidence.

The systems summarized in Figure 7 illustrate why the detection limit should be considered together with the working range and sensing mechanism. For glucose detection, the CuO–graphene/ITO interface exhibited a lower LOD than the PPy–rGO–$(AuNPs–GOD)_4$ electrode, at 1 and 5.6 μM, respectively. However, their reported linear ranges were 1–850 μM and 200–8000 μM, demonstrating different analytical operating windows (Mubarakali et al., 2023; Xu et al., 2010). The lower LOD of the CuO-containing interface therefore does not establish overall superiority: one platform uses non-enzymatic catalysis, whereas the other incorporates glucose oxidase, and their performance was evaluated under study-specific conditions.

The remaining platforms target different analytes and should not be ranked directly against the glucose sensors. Au–PPy, hemoglobin/Au–carbon paste, and montmorillonite–HRP interfaces exhibited LODs of 0.4 μM for xanthine, 0.1 μM for nitric oxide, and 0.6 μM for hydrogen peroxide, respectively (Mubarakali et al., 2023; Devi et al., 2012; Wu et al., 2018). Converting these values into the same unit facilitates presentation but does not remove differences in analyte chemistry, recognition mechanisms, or measurement conditions. Their practical significance depends on the concentration range relevant to the intended application, sample preparation, interference control, and reliable quantification.

Material selection must also account for durability. The Au–PPy sensor exhibited approximately 40% activity loss after 200 uses over 100 days with storage at 4 °C, showing that rapid response and a low initial LOD can coexist with substantial activity loss during use and storage (Devi et al., 2012). Accordingly, Figure 7 provides a descriptive comparison of detection limits and working ranges rather than a universal ranking of material performance. The

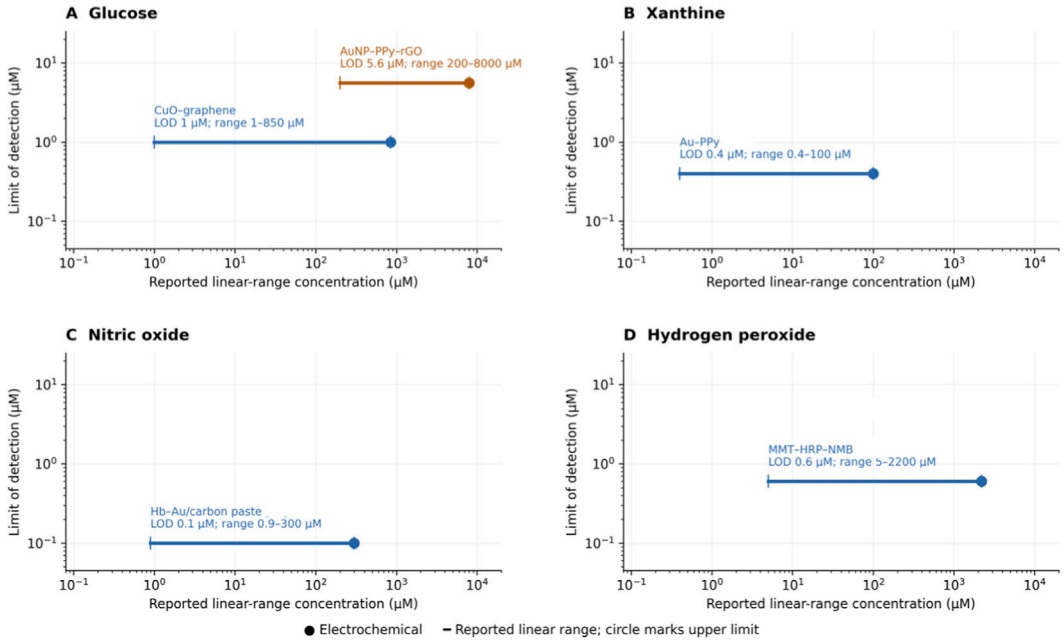


FIGURE 7
Detection limits and linear measurement ranges of representative electrochemical sensing platforms, grouped by target analyte: **(A)** glucose detection using CuO–graphene/ITO (Xu et al., 2010) and PPy–rGO–$(AuNPs–GOD)_4$-modified glassy carbon electrodes (Hepburn et al., 2014); **(B)** xanthine detection using an XOD/Au–PPy/Pt electrode (Yun et al., 2019); **(C)** nitric oxide detection using hemoglobin adsorbed on a gold-colloid-modified carbon paste electrode (Lau et al., 2017); and **(D)** hydrogen peroxide detection using a montmorillonite–horseradish peroxidase–New Methylene Blue N interface (Zhao et al., 2024). The vertical position indicates the LOD, horizontal segments represent the reported linear concentration ranges, and circles mark their upper limits; these segments are not error bars. Both axes use logarithmic scales, and all concentrations are expressed in µM. Data were compiled from the cited studies. Differences in analyte, assay conditions, and sample matrix preclude an overall ranking of material performance across panels.

numerical values and corresponding references are summarized in Table 5.

6 Challenges and future perspectives

A central challenge is preserving colloidal functionality after integration with carbonaceous supports or polymeric matrices. Immobilization can improve particle retention and electrical connectivity while reducing accessible surface area or introducing charge-transfer and diffusion barriers. Consequently, improvements attributed to hybridization require appropriate component-omission controls and measurements that distinguish interfacial kinetics from changes in material loading and analyte transport (Zhao et al., 2008).

Practical limitations include aggregation, chemical transformation, and loss of bioreceptor activity. Aptamer-functionalized AuNPs illustrate the dependence of colloidal stability on surface organization and ionic conditions (Ben Haddada et al., 2018), while copper-based interfaces require assessment of chemical stability under their operating conditions (Velev and Kaler, 1999). Storage-related activity loss in enzyme-containing composites also demonstrates that initial sensitivity does not establish long-term reliability (Xu et al., 2010). Optical systems additionally require evaluation of nonspecific adsorption, sample scattering, and refractive-index variations in complex matrices (Mirshe et al., 2024), (Yun et al., 2019).

Future work should prioritize reproducible fabrication, real-sample validation, and operational and storage stability rather than detection limits alone. Engineered receptors and miniaturized platforms provide opportunities for improved integration (Lau et al., 2017), (Soundharraj et al., 2021), but their durability and scalability require experimental verification. Carbonaceous supports, polymeric coatings, and inorganic spacers should therefore be selected according to a defined interfacial limitation, with both their benefits and associated trade-offs assessed (Table 6).

6.1 *In Situ* and ex situ integration of colloidal nanoparticles

The integration route determines how nanoparticle properties are translated into a functional biosensing interface. A distinction is required between *in situ* nanoparticle formation, in which particles are generated directly on a support, and *ex situ* integration, in which preformed colloids are subsequently immobilized or retained as dispersed assay components. Importantly, electrodeposition is not an unambiguous description of nanoparticle formation: electrochemical reduction of a dissolved metal precursor produces particles *in situ*, whereas electrically assisted deposition of preformed nanoparticles is an *ex situ* assembly process. Both routes have been used in biosensor fabrication (Samanman et al., 2012). Their comparison must therefore consider the starting material and integration mechanism rather than the deposition terminology alone.

TABLE 6 Technical challenges and engineering priorities for colloidal hybrid biosensors.

Technical challenge category	Affected colloidal platform	Underlying physical/chemical cause	Engineering strategy and validation priority	References
Colloidal instability	Aptamer-functionalized AuNPs	Surface organization and ionic conditions influence resistance to aggregation	Optimize receptor coverage and stabilizing coatings; evaluate aggregation under the intended assay conditions	Mubarakali et al. (2023)
Chemical stability	Cu/CuO-containing hybrid electrodes	Surface chemical changes during storage or operation may alter catalytic response	Evaluate protective carbon/polymer interfaces using matched controls; measure chemical integrity and signal retention rather than assuming protection from hybridization	Sabaté del Río et al. (2019)
Bioreceptor activity loss	Enzyme-containing colloidal composites	Storage-related signal loss may reflect enzyme deactivation, component loss, or interfacial changes; the mechanism cannot be established from activity retention alone	Optimize immobilization and storage conditions; distinguish biological activity loss from changes in the supporting matrix	Yun et al. (2019)
Nonspecific adsorption and biofouling	Nanomaterial-modified interfaces exposed to serum or plasma	Adsorption of sample components can obstruct recognition sites and alter electrochemical response	Integrate hydrated antifouling matrices while preserving electrical connectivity; validate performance in complex biological fluids	Zhao et al. (2024)
Optical readout and computational robustness	PRET/LSPR interfaces and AI-assisted SERS platforms	Matrix-dependent optical effects and substrate variability can affect signal interpretation; computational performance depends on the validation design	Use matrix-matched controls and independent substrate batches; evaluate algorithm performance with separated training and test datasets	Wang et al. (2026), Patra and Mishra (2026)
Manufacturing and practical deployment	Quantum-dot biochips and portable AuNP-based assays	Laboratory demonstration does not establish production consistency, shelf life, or performance across sample populations	Assess batch reproducibility, manufacturing yield, storage stability, and independent real-sample validation	Farrokhnia et al. (2022)

The table summarizes potential causes of instability, activity loss, matrix interference, and readout variability, together with strategies for their evaluation. Carbonaceous supports and polymeric matrices should be assessed for both their intended benefits and their effects on accessibility, transport, and signal generation. The listed validation priorities represent requirements for further assessment rather than outcomes demonstrated by every cited study. PRET: plasmon resonance energy transfer; LSPR: localized surface plasmon resonance; SERS: surface-enhanced Raman scattering; AI: artificial intelligence; AuNPs: gold nanoparticles.

For AuNP-modified electrodes, *in situ* reduction of a gold precursor allows nucleation and growth to be adjusted through deposition potential, time, precursor concentration, and substrate preparation. Direct growth can establish electrical contact without requiring a separately added colloidal stabilizer, although deposition additives and subsequent functionalization may still influence the interface. Carbon defects, oxygen-containing groups, and polymer coatings can alter nucleation density and particle distribution. Consequently, the same deposition protocol may produce different architectures on graphene, carbon paste, and polymer-modified electrodes. *In situ* growth also does not guarantee uniform coverage or reproducibility, and electrochemical fabrication conditions may be incompatible with bioreceptors already present on the surface.

The process of *ex situ* synthesis establishes a division between particle creation and device modification work. The process of particle characterization includes size and shape measurements together with concentration levels and surface chemical composition before particles merge into substrates. The drop-casting technique allows for easy material transfer, but its drying process leads to particle aggregation, uneven material distribution, and variable electrode surface contact. The stabilizers that remain after deposition work to maintain dispersion, but residual stabilizers can introduce barriers to electron transfer or restrict receptor accessibility, depending on their chemistry, coverage, and organization. The process of reproducibility depends on two main factors which include colloid synthesis and the process of depositing volume onto substrates and their ability to get wet and the drying process and how particles stay attached. The study showed that the method used to transfer gold nanoparticles onto screen-printed carbon electrodes for SARS-CoV-2 RNA detection served as a major factor that affected the entire manufacturing process.

Preformed AuNPs can also be immobilized through linker-mediated attachment, layer-by-layer assembly, or incorporation into a carbon–polymer composite. In the AuNP-coated QCM interfaces discussed in Section 5.3, self-assembled monolayers provided attachment sites for the particles (Gutiérrez-Santana et al., 2024). Layer-by-layer assembly offers an alternative means of controlling interfacial organization: thiourea-linked AuNP layers on a polytyramine-modified electrode have been investigated for capacitive immunosensing (Zhu et al., 2018). These methods can improve particle retention or spatial organization, but molecular linkers and polymer layers may introduce charge-transfer or diffusion barriers. Mechanical incorporation into carbon paste provides another integration route, although embedding particles does not ensure that all of them remain accessible to the sample or electrically connected to the exposed sensing surface.

Carbon and polymer components therefore mediate the trade-off between particle stabilization and transduction. Carbonaceous supports can establish conductive pathways and distribute particles, whereas polymeric matrices can retain particles, present functional groups, and regulate permeability. However, carbon restacking, insulating binders, excessive polymer thickness, or strongly bound ligands can reduce the fraction of accessible sites. The choice between *in situ* and *ex situ* integration should consequently be evaluated using matched interfaces rather than assuming that either route is intrinsically superior. Relevant comparisons include particle loading, electrochemically accessible area, receptor coverage, charge-transfer behavior, response time, device-to-device variation, and signal retention after storage or washing. For optical interfaces, particle spacing and aggregation additionally influence plasmonic coupling; for acoustic interfaces, hydration and film mechanics affect the measured response.

Magnetic nanoparticles introduce a different configuration because target capture can occur in suspension before the recognition complex reaches the transducer. Antibodies, aptamers, or peptides attached to the particle surface enable target association, followed by magnetic separation and resuspension in a smaller volume or a more suitable measurement medium. The magnetic component provides manipulation, while an outer carbon, silica, or polymer layer can supply functional groups and modify interactions with the sample. These coatings must nevertheless be assessed for their effects on particle aggregation, capture-site accessibility, and nonspecific adsorption. An experimental example combined antibody-functionalized Fe_3O_4@SiO_2 capture particles with a graphene-supported Au@Pt detection assembly for *Escherichia coli* O157 (Freko et al., 2024). This architecture separates magnetic capture from carbon-supported signal generation. Capture efficiency, recovery after separation, and the contribution of each component are required to establish its advantage over a nonmagnetic or nonhybrid assay.

Dispersed colloids are also applicable to emerging sensing formats without permanent immobilization on a solid transducer. AuNP aggregation assays and lateral-flow reporters provide established examples, while single-impact electrochemistry uses transient particle–electrode encounters to generate discrete signals. A CRISPR/Cas12a assay combined DNA-functionalized AgNP reporters, magnetic separation, and single-impact electrochemical detection, demonstrating how solution-phase recognition can be coupled to particle counting without target amplification (Guo et al., 2023). A further example coupled a CRISPR-responsive DNA hydrogel with AgNP-based nano-impact electrochemistry (Zakiyyah et al., 2025). These systems illustrate complementary functions for a hydrated molecular network and a colloidal reporter rather than a conventional nanoparticle-coated electrode. Their limitations include spontaneous reporter release, particle stability, transport to the electrode, and variability in the probability of detecting individual particles.

Overall, the relevant design choice is whether colloidal functionality is best retained through direct growth, controlled immobilization, composite incorporation, or operation in suspension. Carbon–polymer–colloid integration is advantageous only when its contribution to connectivity, retention, recognition, or transport is demonstrated against appropriate controls. Neither a lower detection limit nor a larger signal alone establishes a beneficial interfacial interaction (Table 7).

6.2 Research gaps and priorities for practical translation

The central research gap is the incomplete understanding of how colloidal functionality changes during integration into carbon–polymer sensing interfaces. Properties measured in dispersion cannot be assumed to persist after immobilization (Hepburn et al., 2014). Ligands that suppress aggregation may restrict electron transfer or receptor coupling, while drying and matrix incorporation can change particle spacing and accessible surface area (Zhao et al., 2008) (Grys et al., 2021). Similarly, a polymer that improves particle retention may obstruct analyte transport, and nanoparticle loading that increases signal may also increase background or coating heterogeneity. The key question is therefore not whether hybridization improves sensitivity, but which interfacial properties are preserved, compromised, or newly introduced during device fabrication (Zhao et al., 2008) (Grys et al., 2021).

Addressing this gap requires linked characterization before and after integration. Dispersion measurements should be connected with particle distribution, coating thickness, electrical contact, analyte accessibility, and receptor activity in the final device. Component-omission controls and matched material loadings are needed to distinguish specific interactions from changes in surface area or reporter quantity (Zhao et al., 2008; Grys et al., 2021). In particular, the relationships between polymer composition, nanoparticle/polymer ratio, film structure, and analytical response require systematic investigation rather than optimization of one fabrication variable at a time (Hepburn et al., 2014; Zhao et al., 2008; Grys et al., 2021).

Scalable fabrication remains a separate unresolved challenge. Future studies should determine whether the selected architecture can be reproduced across independent material batches and devices, reporting fabrication yield, loading variation, coating uniformity, and calibration variability. Translation from manual deposition to printing, spraying, or automated assembly should be evaluated for its effects on particle organization and receptor function rather than assumed to preserve laboratory performance.

Real-matrix validation should establish whether the interface remains selective and quantitatively reliable after exposure to the intended sample. Spiked-sample recovery should be distinguished from measurement of endogenous analytes, with dilution, pretreatment, interfering species, and agreement with a reference method reported explicitly. Likewise, stability assessment should distinguish colloidal aggregation, storage-related activity loss, operational drift, and regeneration performance. These measurements are necessary to identify whether failure originates from the particles, matrix, receptor, or their interfaces.

Commercial translation ultimately requires an application-specific balance between analytical performance, manufacturing consistency, shelf life, sample handling, and readout complexity. Priority should therefore be given to the simplest architecture that meets a defined analytical need with reproducible performance in the intended matrix. This framework provides a basis for future studies that connect colloid-to-device transformation with measurable fabrication and validation outcomes, rather than

TABLE 7 Comparison of *in situ* nanoparticle formation, *ex situ* colloidal integration, and suspension-based biosensing configurations.

Criterion	*In situ* growth on the transducer	*Ex situ* colloids immobilized on the transducer	Suspension-based colloids
Synthesis control	Growth is adjusted through precursor concentration, deposition conditions, and substrate properties (Samanman et al., 2012)	Particle preparation precedes device modification; transfer conditions introduce additional fabrication variables (Samanman et al., 2012; Belding et al., 2009)	Particle preparation precedes conjugation and assay assembly (Guo et al., 2023; Zakiyyah et al., 2025)
Carbon/polymer interaction	Support chemistry and pre-existing surface layers influence particle formation and subsequent functionalization (Samanman et al., 2012)	Linker-mediated assembly and polymer-containing interfaces determine attachment and accessibility (Zhu et al., 2018)	Functional coatings and responsive networks regulate particle organization, recognition, or release (Guo et al., 2023; Zakiyyah et al., 2025)
Signal transduction	Depends on the resulting nanoparticle–electrode interface and subsequent bioreceptor immobilization (Samanman et al., 2012)	Depends on particle distribution, surface coverage, and the assembled sensing architecture (Zhu et al., 2018; Belding et al., 2009)	Depends on capture/release efficiency and coupling of the dispersed reporter to the readout (Guo et al., 2023; Zakiyyah et al., 2025)
Bioreceptor integration	Can follow nanoparticle growth and surface activation (Samanman et al., 2012)	Can be performed after nanoparticle assembly; the sequence depends on the fabrication protocol (Zhu et al., 2018)	Recognition elements or molecular linkers are attached to dispersed particles before assay operation (Zhu et al., 2018; Guo et al., 2023)
Reproducibility variables	Electrode preparation and nanoparticle deposition conditions (Samanman et al., 2012)	Colloid preparation, deposition method, surface coverage, and layer assembly (Zhu et al., 2018; Belding et al., 2009)	Conjugation, magnetic separation, reporter release, and—for single-impact methods—particle arrival and detection (Freko et al., 2024; Guo et al., 2023; Zakiyyah et al., 2025)
Main limitation	Performance remains dependent on the fabricated interface; superiority over *ex situ* methods requires matched comparisons (Samanman et al., 2012)	Analytical performance is sensitive to transfer and assembly conditions (Zhu et al., 2018; Belding et al., 2009)	Incomplete capture or separation, background reporter release, and transport-limited particle detection require evaluation (Freko et al., 2024; Guo et al., 2023; Zakiyyah et al., 2025)
Useful validation	Deposition reproducibility and comparison with appropriate control electrodes (Samanman et al., 2012)	Surface characterization, device-to-device variation, and comparison of deposition methods (Zhu et al., 2018; Belding et al., 2009)	Capture recovery, negative controls, matrix effects, and readout efficiency, as applicable (Freko et al., 2024; Guo et al., 2023; Zakiyyah et al., 2025)

treating increasingly complex material combinations as evidence of progress.

6.3 Validation and reproducibility of AI-Assisted biosensing

AI-assisted SERS should be assessed according to the independence and diversity of its validation data rather than classification accuracy alone. Dataset reporting should distinguish the numbers of independent patients or samples, substrate batches, and spectra per sample. Repeated spectra from one specimen do not constitute independent biological observations. Training, validation, and test partitions should therefore be separated at the sample or patient level; batch-separated testing is additionally needed to assess fabrication-dependent effects. Preprocessing, feature selection, data augmentation, and hyperparameter optimization should be restricted to the training workflow to prevent information leakage (Varma and Simon, 2006; Gurian et al., 2021; Lilek et al., 2025; Xiu et al., 2012).

Overfitting should be evaluated through learning curves, appropriate cross-validation, and comparison with simpler baseline models. External validation should use independently collected samples, preferably involving different measurement sessions, operators, or instruments. Transferability between substrates requires particular attention because changes in nanoparticle organization, surface coatings, and electromagnetic enhancement can alter spectral distributions. Performance should therefore be evaluated across independently fabricated batches and alternative substrates, with any recalibration or model adaptation explicitly reported (Varma and Simon, 2006; Gurian et al., 2021; Lilek et al., 2025; Xiu et al., 2012).

Model interpretability should connect influential spectral regions with plausible molecular features while considering substrate, background, and preprocessing artifacts. Reproducibility requires sufficient information on sample preparation, spectral acquisition, data partitions, preprocessing, software, and model settings. For classification, sensitivity, specificity, class balance, and confidence intervals should accompany accuracy; quantitative prediction additionally requires independent concentration standards and prediction-error metrics. Consequently, the reported performance of the ZADA platform (Soundharraj et al., 2021) should be interpreted within its evaluated dataset rather than as evidence of universal diagnostic reliability.

Computational receptor design presents a separate validation requirement. The use of a designed miniprotein (Farrokhnia et al., 2022) does not itself demonstrate greater stability than an antibody. Binding specificity, activity retention, immobilization effects, and

storage performance require experimental comparison under matched conditions.

6.4 Safety, environmental release, and sustainable fabrication

The practical translation of carbon–polymer–colloid biosensors requires evaluation of material safety alongside analytical performance. Toxicological findings should be interpreted according to particle composition, dose, surface chemistry, exposure duration, and intended use. For AgNPs, Xiu et al. demonstrated that antibacterial activity under their experimental conditions depended on oxidative Ag^+ release; this finding highlights the importance of dissolution measurements but does not establish safety in mammalian systems (Derfus et al., 2004). For Cd-containing quantum dots, Derfus et al. linked cytotoxicity to nanocrystal deterioration and cadmium release, demonstrating why core composition and coating integrity require consideration (Boyadzhiev et al., 2021). Cu/CuO systems also require assessment of both particulate and dissolved species: studies of CuO exposure indicate that extracellular dissolution alone does not fully explain cellular toxicity (Bagheri et al., 2017). Consequently, safety claims cannot be transferred directly between different nanoparticle formulations or exposure models.

For immobilized sensing interfaces, a priority is determining whether nanoparticles, dissolved metals, or coating fragments are released during sample contact, washing, regeneration, and disposal. Future studies should distinguish particulate release from dissolved-ion release and relate both to the initial material loading and changes in analytical response. Carbon coatings and polymer entrapment should therefore be evaluated for retention efficiency rather than assumed to prevent environmental release. Exposure assessment should also reflect the device format, distinguishing enclosed disposable assays from wearable or implantable interfaces.

Polymer selection introduces a further lifecycle consideration. A biodegradable designation does not establish rapid degradation under the conditions encountered after disposal. Bagheri et al. demonstrated different degradation behaviours among polymers, including PCL, during controlled freshwater and seawater exposure (Pourzahedi and Eckelman, 2015). Moreover, polymer fragmentation should be distinguished from complete biodegradation, and degradation of the organic matrix does not establish elimination of its inorganic fillers. Hybrid coatings should therefore be assessed for both matrix degradation and the subsequent fate of retained or released nanoparticles.

Green synthesis and sustainable electrode fabrication should similarly be supported by process-level evidence. Comparative lifecycle assessment of AgNP synthesis routes shows why precursor production, reagents, energy demand, and functional performance must be considered together (Zikulnig et al., 2025). Biomass-derived reducing agents alone are therefore insufficient evidence of a lower overall environmental burden. For printed sensing devices, lifecycle assessment provides a framework for evaluating substrate selection, conductive materials, manufacturing, and end-of-life treatment [141]. Priorities for future biosensor development include reducing unnecessary material loading, solvent consumption, and processing energy while maintaining reproducibility and analytical reliability. Environmental comparisons should ideally use a common functional basis, such as one validated assay, and account for shelf life, failed measurements, and any demonstrated reuse.

7 Conclusion

Colloidal materials have considerable potential in biosensor technologies owing to their sensitivity, selectivity, and multifunctional integration. The optoelectronic properties of PbS quantum dots, along with the functionalizable surface chemistry of SiO_2 and the complementary dielectric and plasmonic functions of SiO_2–Ag hybrids, as well as the extensive surface area and ion-exchange capacity of clay colloids such as montmorillonite, facilitate the precise detection of biological targets. Furthermore, integrating hybrid Surface-Enhanced Raman Spectroscopy (SERS)-based platforms, such as ZnO-Au, with AI-assisted analysis introduces a novel approach to the application of colloidal systems in molecular diagnostics. Overall, colloidal materials constitute a rapidly advancing area of research within biosensors and are strategically positioned to contribute significantly to the development of high-performance, cost-effective, and sustainable sensors for clinical diagnosis, environmental monitoring, food safety, and biomedical analysis. Ongoing research efforts are essential to addressing existing challenges, including physical stability, biocompatibility, and scalable production, thereby fostering the development of more reliable and broadly applicable biosensor platforms.

Author contributions

HA: Conceptualization, Data curation, Formal Analysis, Investigation, Methodology, Project administration, Resources, Software, Validation, Visualization, Writing – original draft, Writing – review and editing. FC: Conceptualization, Data curation, Formal Analysis, Funding acquisition, Investigation, Methodology, Project administration, Resources, Software, Supervision, Validation, Visualization, Writing – original draft, Writing – review and editing. EÖ: Conceptualization, Data curation, Formal Analysis, Investigation, Methodology, Project administration, Resources, Software, Supervision, Validation, Visualization, Writing – original draft, Writing – review and editing. JR: Conceptualization, Data curation, Formal Analysis, Funding acquisition, Investigation, Methodology, Project administration, Resources, Software, Validation, Visualization, Writing – original draft, Writing – review and editing.

Funding

The author(s) declared that financial support was not received for this work and/or its publication.

Conflict of interest

The author(s) declared that this work was conducted in the absence of any commercial or financial relationships that could be construed as a potential conflict of interest.

Generative AI statement

The author(s) declared that generative AI was used in the creation of this manuscript. The authors acknowledge the use of artificial intelligence (AI)- assisted tools for language editing, grammatical improvement, and the preparation of schematic figures in this manuscript. Some illustrations were created with the assistance of AI-based tools and Microsoft PowerPoint. All scientific content, interpretations, and conclusions were reviewed and approved by the authors

Any alternative text (alt text) provided alongside figures in this article has been generated by Frontiers with the support of artificial intelligence and reasonable efforts have been made to ensure accuracy, including review by the authors wherever possible. If you identify any issues, please contact us.

Publisher's note

All claims expressed in this article are solely those of the authors and do not necessarily represent those of their affiliated organizations, or those of the publisher, the editors and the reviewers. Any product that may be evaluated in this article, or claim that may be made by its manufacturer, is not guaranteed or endorsed by the publisher.

References

Ahmad, R., Tripathy, N., Ahn, M.-S., Bhat, K. S., Mahmoudi, T., and Wang, Y. (2017). Highly efficient non-enzymatic glucose sensor based on CuO modified vertically-grown ZnO nanorods on electrode. *Sci. Rep.* 7, 5715. doi: 10.1038/s41598-017-06064-8

Akkad, H., and Ahlatcıoğlu Özerol, E. (2026). Overview of hydrocolloid polymeric materials for biomedical applications: a review. *Int. J. Polym. Mater. Polym. Biomaterials* 75, 302–324. doi: 10.1080/00914037.2025.2528667

Akkad, H., Ciftci, F., Ahlatcıoğlu Özerol, E., and Kizilkurtlu, A. A. (2026). From static to dynamic: the convergence of nanomaterials and 3D/4D bioprinting for adaptive wearable sports biosensors. *Biosens. (Basel)* 16, 392. doi: 10.3390/bios16070392

Al-Gethami, W., Alhashmialameer, D., Al-Qasmi, N., Ismail, S. H., and Sadek, A. H. (2022). Design of a novel nanosensors based on green synthesized CoFe2O4/Ca-Alginate nanocomposite-coated QCM for rapid detection of Pb(II) ions. *Nanomater. (Basel)* 12, 3620. doi: 10.3390/nano12203620

Ali, A. A., Altemimi, A. B., Alhelfi, N., and Ibrahim, S. A. (2020). Application of biosensors for detection of pathogenic food bacteria: a review. *Biosens. (Basel)* 10, 58. doi: 10.3390/bios10060058

Animashaun, C., Lahcen, A. A., and Slaughter, G. (2025). Gold nanoparticle-enhanced molecularly imprinted polymer electrode for non-enzymatic lactate sensing. *Biosens. (Basel)* 15, 384. doi: 10.3390/bios15060384

Bagheri, A. R., Laforsch, C., Greiner, A., and Agarwal, S. (2017). Fate of so-called biodegradable polymers in seawater and freshwater. *Glob. Challenges* 1, 1700048. doi: 10.1002/gch2.201700048

Belding, S. R., Dickinson, E. J. F., and Compton, R. G. (2009). Diffusional cyclic voltammetry at electrodes modified with random distributions of electrocatalytic nanoparticles: theory. *J. Phys. Chem. C* 113, 11149–11156. doi: 10.1021/jp901664p

Ben Haddada, M., Salmain, M., and Boujday, S. (2018). Gold colloid-nanostructured surfaces for enhanced piezoelectric immunosensing of staphylococcal enterotoxin A. *Sens. Actuators B Chem.* 255, 1604–1613. doi: 10.1016/j.snb.2017.08.180

Boyadzhiev, A., Avramescu, M.-L., Wu, D., Williams, A., Rasmussen, P., and Halappanavar, S. (2021). Impact of copper oxide particle dissolution on lung epithelial cell toxicity: response characterization using global transcriptional analysis. *Nanotoxicology* 15, 380–399. doi: 10.1080/17435390.2021.1872114

Campanile, R., Acunzo, A., Scardapane, E., Minopoli, A., Martins, V. C., Di Girolamo, R., et al. (2022). Multifunctional core@satellite magnetic particles for magnetoresistive biosensors. *ACS Omega* 7, 36543–36550. doi: 10.1021/acsomega.2c04442

Carvalho, A. P. G., Alegria, ECBA, Fantoni, A., Ferraria, A. M., do Rego, A. M. B., and Ribeiro, A. P. C. (2022). Effect of graphene vs. reduced graphene oxide in gold nanoparticles for optical biosensors—A comparative study. *Biosens. (Basel)* 12, 163. doi: 10.3390/bios12030163

Chapter 1 General Chemistry of Silica (1979). 1–14. doi: 10.1016/S0301-4770(08)60805-2

Chaturvedi, A., Tripathi, D., and Ranjan, R. (2025). Nano-enabled biosensors in early detection of plant diseases. *Front. Nanotechnol.* 7, 1545792. doi: 10.3389/fnano.2025.1545792

Chen, H.-C, Su, W.-R., and Yeh, Y.-C. (2020). Functional Channel of SWCNTs/Cu2O/ZnO NRs/graphene hybrid electrodes for highly sensitive nonenzymatic glucose sensors. *ACS Appl. Mater. Interfaces* 12 (29), 32905–32914. doi: 10.1021/acsami.0c07943

Chen, C., Liu, Y., Zhang, K., Fan, Q., Luo, T., Peng, S., et al. (2026). An enzyme-free flexible and wearable sensor based on PEDOT/CNTs/Au for continuous detection of glucose in sweat. *Colloids Surf. A Physicochem Eng. Asp.* 728, 138696. doi: 10.1016/j.colsurfa.2025.138696

Damborský, P., Švitel, J., and Katrlík, J. (2016). Optical biosensors. *Essays Biochem.* 60, 91–100. doi: 10.1042/EBC20150010

Derfus, A. M., Chan, W. C. W., and Bhatia, S. N. (2004). Probing the cytotoxicity of semiconductor quantum dots. *Nano Lett.* 4, 11–18. doi: 10.1021/nl0347334

Devi, R., Yadav, S., and Pundir, C. S. (2012). Au-colloids–polypyrrole nanocomposite film based xanthine biosensor. *Colloids Surf. A Physicochem Eng. Asp.* 394, 38–45. doi: 10.1016/j.colsurfa.2011.11.021

Dyussembayev, K., Sambasivam, P., Bar, I., Brownlie, J. C., Shiddiky, M. J. A., and Ford, R. (2021). Biosensor technologies for early detection and quantification of plant pathogens. *Front. Chem.* 9, 636245. doi: 10.3389/fchem.2021.636245

Farrokhnia, M., Amoabediny, G., Ebrahimi, M., Ganjali, M., and Arjmand, M. (2022). Ultrasensitive early detection of insulin antibody employing novel electrochemical nano-biosensor based on controllable electro-fabrication process. *Talanta* 238, 122947. doi: 10.1016/j.talanta.2021.122947

Freko, S., Nikić, M., Mayer, D., Weiß, L. J. K., Simmel, F. C., and Wolfrum, B. (2024). Digital CRISPR-powered biosensor concept without target amplification using single-impact electrochemistry. *ACS Sens.* 9, 6197–6206. doi: 10.1021/acssensors.4c02060

Fu, Y., Liu, T., Wang, H., Wang, Z., Hou, L., Jiang, J., et al. (2024). Applications of nanomaterial technology in biosensing. *J. Sci. Adv. Mater. Devices* 9, 100694. doi: 10.1016/j.jsamd.2024.100694

Geng, H., Vilms Pedersen, S., Ma, Y., Haghighi, T., Dai, H., Howes, P. D., et al. (2022). Noble metal nanoparticle biosensors: from fundamental studies toward Point-of-Care diagnostics. *Acc. Chem. Res.* 55, 593–604. doi: 10.1021/acs.accounts.1c00598

German, N., Popov, A., Ramanavicius, A., and Ramanaviciene, A. (2022). Development and practical application of glucose biosensor based on dendritic gold nanostructures modified by conducting polymers. *Biosens. (Basel)* 12, 641. doi: 10.3390/bios12080641

Grys, D., Chikkaraddy, R., Kamp, M., Scherman, O. A., Baumberg, J. J., and de Nijs, B. (2021). Eliminating irreproducibility in SERS substrates. *J. Raman Spectrosc.* 52, 412–419. doi: 10.1002/jrs.6008

Guo, J., Zhu, Y., and Miao, P. (2023). Nano-impact electrochemical biosensing based on a CRISPR-responsive DNA hydrogel. *Nano Lett.* 23, 11099–11104. doi: 10.1021/acs.nanolett.3c03448

Gurian, E., Di Silvestre, A., Mitri, E., Pascut, D., Tiribelli, C., Giuffrè, M., et al. (2021). Repeated double cross-validation applied to the PCA-LDA classification of SERS spectra: a case study with serum samples from hepatocellular carcinoma patients. *Anal. Bioanal. Chem.* 413, 1303–1312. doi: 10.1007/s00216-020-03093-7

Gutiérrez-Santana, J. C., Rosas-Espinosa, V., Martinez, E., Casiano-García, E., and Coria-Jiménez, V. R. (2024). Metal nanoparticle-based biosensors for the early diagnosis of infectious diseases caused by ESKAPE pathogens in the fight against the antimicrobial-resistance crisis. *Biosens. (Basel)* 14, 339. doi: 10.3390/bios14070339

Hasan, M. R., Niebuur, B.-J., Siebrecht, M., Kuttich, B., Schweins, R., Widmer-Cooper, A., et al. (2023). The colloidal stability of apolar nanoparticles in solvent mixtures. *ACS Nano* 17, 9302–9312. doi: 10.1021/acsnano.3c00812

He, Z., Zhang, J., Kuang, S., Li, S., Wang, Y., Ding, J., et al. (2025). Colloidal gold technology in viral diagnostics: recent innovations, clinical applications, and future perspectives. *Virology* 612, 110686. doi: 10.1016/j.virol.2025.110686

Hemdan, M., Ali, M. A., Doghish, A. S., Mageed, S. S. A., Elazab, I. M., Khalil, M. M., et al. (2024). Innovations in biosensor technologies for healthcare diagnostics and therapeutic drug monitoring: applications, recent progress, and future research challenges. *Sensors* 24, 5143. doi: 10.3390/s24165143

Hepburn, W. G., Batchelor-McAuley, C., Tschulik, K., Barnes, E. O., Kachoosangi, R. T., and Compton, R. G. (2014). Diffusional transport to and through thin-layer nanoparticle film modified electrodes: capped CdSe nanoparticle modified electrodes. *Phys. Chem. Chem. Phys.* 16, 18034–18041. doi: 10.1039/C4CP02440K

Heydari, S., and Haghayegh, G. H. (2014). Application of nanoparticles in quartz crystal microbalance biosensors. *J. Sens. Technol.* 04, 81–100. doi: 10.4236/jst.2014.42009

Huang, C., Wen, T., Shi, F.-J., Zeng, X.-Y., and Jiao, Y.-J. (2020). Rapid detection of IgM antibodies against the SARS-CoV-2 virus via colloidal gold nanoparticle-based lateral-flow assay. *ACS Omega* 5, 12550–12556. doi: 10.1021/acsomega.0c01554

Huang, C.-W., Lin, C., Nguyen, M. K., Hussain, A., Bui, X.-T., and Ngo, H. H. (2023). A review of biosensor for environmental monitoring: principle, application, and corresponding achievement of sustainable development goals. *Bioengineered* 14, 58–80. doi: 10.1080/21655979.2022.2095089

Jhuang, L.-S., Kumar, G., and Chen, F.-C. (2021). Localized surface plasmon resonance of copper nanoparticles improves the performance of quasi-two-dimensional perovskite light-emitting diodes. *Dyes Pigments* 188, 109204. doi: 10.1016/j.dyepig.2021.109204

Kim, M. G., Jue, M., Lee, K. H., Lee, E. Y., Roh, Y., Lee, M., et al. (2023). Deep learning assisted surface-enhanced raman spectroscopy (SERS) for rapid and direct nucleic acid amplification and detection: toward enhanced molecular diagnostics. *ACS Nano* 17, 18332–18345. doi: 10.1021/acsnano.3c05633

Koedrith, P., Thasiphu, T., Weon, J.-I., Boonprasert, R., Tuitemwong, K., and Tuitemwong, P. (2015). Recent trends in rapid environmental monitoring of pathogens and toxicants: potential of nanoparticle-based biosensor and applications. *Sci. World J.* 2015, 510982. doi: 10.1155/2015/510982

Kress, S. J. P., Richner, P., Jayanti, S. V., Galliker, P., Kim, D. K., Poulikakos, D., et al. (2014). Near-field light design with colloidal quantum dots for photonics and plasmonics. *Nano Lett.* 14, 5827–5833. doi: 10.1021/nl5026997

Kuntoji, G., Kousar, N., Gaddimath, S., and Koodlur Sannegowda, L. (2024). Macromolecule–nanoparticle-based hybrid materials for biosensor applications. *Biosens. (Basel)* 14, 277. doi: 10.3390/bios14060277

Lim, H. J., Jin, H., Chua, B., and Son, A. (2022). Clustered detection of eleven phthalic acid esters by fluorescence of graphene quantum dots displaced from gold nanoparticles. *ACS Appl. Mater Interfaces* 14, 4186–4196. doi: 10.1021/acsami.1c21756

Lau, H. Y., Wu, H., Wee, E. J. H., Trau, M., Wang, Y., and Botella, J. R. (2017). Specific and sensitive isothermal electrochemical biosensor for plant pathogen DNA detection with colloidal gold nanoparticles as probes. *Sci. Rep.* 7, 38896. doi: 10.1038/srep38896

Lei, C., Zhang, Z., Liu, H., Kong, J., and Deng, J. (1996). Biosensoring of hydrogen peroxide using new methylene blue N incorporated in a montmorillonite-modified horseradish peroxidase immobilization matrix as an electron shuttle. *Anal. Chim. Acta* 332, 73–81. doi: 10.1016/0003-2670(96)82792-9

Li, W., Huberman-Shlaes, J., and Tian, B. (2023). Perspectives on multiscale colloid-based materials for biomedical applications. *Langmuir* 39, 13759–13769. doi: 10.1021/acs.langmuir.3c01274

Lilek, D., Zimmermann, D., Steininger, L., Musso, M., Wilts, B. D., Gamsjaeger, S., et al. (2025). Machine learning of raman spectroscopic data: Comparison of different validation strategies. *J. Raman Spectrosc.* 56, 867–877. doi: 10.1002/jrs.6842

Liu, S., and Ju, H. (2003). Nitrite reduction and detection at a carbon paste electrode containing hemoglobin and colloidal gold. *Analyst* 128, 1420–1424. doi: 10.1039/b310100b

Luppa, P. B., Müller, C., Schlichtiger, A., and Schlebusch, H. (2011). Point-of-care testing (POCT): current techniques and future perspectives. *TrAC Trends Anal. Chem.* 30, 887–898. doi: 10.1016/j.trac.2011.01.019

Ma, Q., Li, Y., and Su, X. (2015). Silica-nanobead-based sensors for analytical and bioanalytical applications. *TrAC Trends Anal. Chem.* 74, 130–145. doi: 10.1016/j.trac.2015.06.006

Malathi, S., Pakrudheen, I., Kalkura, S. N., Webster, T. J., and Balasubramanian, S. (2022). Disposable biosensors based on metal nanoparticles. *Sensors Int.* 3, 100169. doi: 10.1016/j.sintl.2022.100169

Mirshekari, H., Dabirmanesh, B., Daneshjou, S., and Khajeh, K. (2024). Fabrication and evaluation of a plasmonic biosensor based on silica-coated gold nanorods for highly-sensitive detection of Anti-Müllerian hormone. *Colloid Interface Sci. Commun.* 61, 100795. doi: 10.1016/j.colcom.2024.100795

Mondal, R., Dam, P., Chakraborty, J., Paret, M. L., Katı, A., Altuntas, S., et al. (2022). Potential of nanobiosensor in sustainable agriculture: the state-of-art. *Heliyon* 8, e12207. doi: 10.1016/j.heliyon.2022.e12207

Moyano, A., Serrano-Pertierra, E., Salvador, M., Martínez-García, J., Piñeiro, Y., Yañez-Vilar, S., et al. (2020). Carbon-coated superparamagnetic nanoflowers for biosensors based on lateral flow immunoassays. *Biosens. (Basel)* 10, 80. doi: 10.3390/bios10080080

Mubarakali, A., Gopinath, S., Parthasarathy, P., Arun Kumar, U., and Alavudeen Basha, A. (2023). Highly efficient and sensitive non-enzymatic glucose biosensor based on flower-shaped CuO-colloid nanoparticles decorated with graphene-modified nanocomposite electrode. *Measurement* 217, 113145. doi: 10.1016/j.measurement.2023.113145

Naresh, V., and Lee, N. (2021). A review on biosensors and recent development of nanostructured materials-enabled biosensors. *Sensors (Basel)* 21, 1109. doi: 10.3390/s21041109

Nath, P., and Ray, A. (2023). Nanotechnology-based strategies for advancing point-of-care lateral flow immunoassays. *Curr. Opin. Biomed. Eng.* 28, 100504. doi: 10.1016/j.cobme.2023.100504

Pan, X., Zhang, Z., and Su, M. (2024). Colloidal self-assembly in biosensing strategies for biomarkers diagnosis. *Innov. Mater.* 2, 100076. doi: 10.59717/j.xinn-mater.2024.100076

Parihar, M., Mazumder, N.W. N. N, Sahana, B. R., Dehury, B., and Mazumder, N. (2025). Point-of-care biosensors for infectious disease diagnosis: recent updates and prospects. *RSC Adv.* 15, 29267–29283. doi: 10.1039/D5RA03897A

Patra, S. R., and Mishra, S. P. (2026). Comprehensive comparative evaluation of methylene blue adsorption on pristine and ZnCl2 modified montmorillonite K10. *Discov. Appl. Sci.* 8, 922. doi: 10.1007/s42452-026-08885-7

Pourzahedi, L., and Eckelman, M. J. (2015). Comparative life cycle assessment of silver nanoparticle synthesis routes. *Environ. Sci. Nano* 2, 361–369. doi: 10.1039/C5EN00075K

Ramesh, M., Janani, R., Deepa, C., and Rajeshkumar, L. (2022). Nanotechnology-enabled biosensors: a review of fundamentals, design principles, materials, and applications. *Biosens. (Basel)* 13, 40. doi: 10.3390/bios13010040

Reyes, P. I., Zhang, Z., Chen, H., Duan, Z., Zhong, J., Saraf, G., et al. (2009). A ZnO nanostructure-based quartz crystal microbalance device for biochemical sensing. *IEEE Sens. J.* 9, 1302–1307. doi: 10.1109/JSEN.2009.2030250

Rovira-Más, F., Saiz-Rubio, V., and Cuenca-Cuenca, A. (2021). Sensing architecture for terrestrial crop monitoring: harvesting data as an asset. *Sensors (Basel)* 21, 3114. doi: 10.3390/s21093114

Sabaté del Río, J., Henry, O. Y. F., Jolly, P., and Ingber, D. E. (2019). An antifouling coating that enables affinity-based electrochemical biosensing in complex biological fluids. *Nat. Nanotechnol.* 14, 1143–1149. doi: 10.1038/s41565-019-0566-z

Samanman, S., Kanatharana, P., Asawatreratanakul, P., and Thavarungkul, P. (2012). Characterization and application of self-assembled layer by layer gold nanoparticles for highly sensitive label-free capacitive immunosensing. *Electrochim Acta* 80, 202–212. doi: 10.1016/j.electacta.2012.07.016

Shanbhag, M. M., Manasa, G., Mascarenhas, R. J., Mondal, K., and Shetti, N. P. (2023). Fundamentals of bio-electrochemical sensing. *Chem. Eng. J. Adv.* 16, 100516. doi: 10.1016/j.ceja.2023.100516

Shaw, D. S., and Honeychurch, K. C. (2022). Nanosensor applications in plant science. *Biosens. (Basel)* 12, 675. doi: 10.3390/bios12090675

Shukla, N., Chetri, P., Boruah, R., Gogoi, A., and Ahmed, G. A. (2022). "*Surface Plasmon Resonance Biosensors Based on Kretschmann Configuration: Basic Instrumentation and Applications*". in Recent Advances in Plasmonic Probes. Editors R. Biswas and N. Mazumder (Cham, Switzerland: Springer). doi: 10.1007/978-3-030-99491-4_6

Simoska, O., Duay, J., and Stevenson, K. J. (2020). Electrochemical detection of multianalyte biomarkers in wound healing efficacy. *ACS Sens.* 5, 3547–3557. doi: 10.1021/acssensors.0c01697

Skládal, P. (2024). Piezoelectric biosensors: shedding light on principles and applications. *Mikrochim. Acta* 191, 184. doi: 10.1007/s00604-024-06257-9

Song, M., Lin, X., Peng, Z., Xu, S., Jin, L., Zheng, X., et al. (2021). Materials and methods of biosensor interfaces with stability. *Front. Mater* 7, 583739. doi: 10.3389/fmats.2020.583739

Soundharraj, P., Dhinasekaran, D., Aruna, P., and Ganesan, S. (2021). Facile synthesis of biomass silica-silver colloidal nanoparticles and its application as highly sensitive fluorescent biosensor. *Surfaces Interfaces* 23, 101010. doi: 10.1016/j.surfin.2021.101010

Sreejith, S., Leo Joseph, L. M. I., Kollem, S., Vijumon, V. T., and Ajayan, J. (2023). Biodegradable sensors: a comprehensive review. *Measurement* 219, 113261. doi: 10.1016/j.measurement.2023.113261

Swain, J., Swain, S., Singh, D., Jena, A., Samantaray, R., and Sahu, R. (2023). "Role of piezoelectric biosensors," in *Point-Of-Care Biosensors for Infectious Diseases*. Wiley, 129–145. doi: 10.1002/9783527837946.ch7

Tanner, E. E. L., Sokolov, S. V., Young, N. P., and Compton, R. G. (2017). DNA capping agent control of electron transfer from silver nanoparticles. *Phys. Chem. Chem. Phys.* 19, 9733–9738. doi: 10.1039/C7CP01721A

Vaidya, R., Atanasov, P., and Wilkins, E. (1995). Effect of interference on the performance of glucose enzyme electrodes using nafion ® coatings. *Med. Eng. Phys.* 17, 416–424. doi: 10.1016/1350-4533(94)00006-U

Varma, S., and Simon, R. (2006). Bias in error estimation when using cross-validation for model selection. *BMC Bioinforma.* 7, 91. doi: 10.1186/1471-2105-7-91

Velev, O. D., and Kaler, E. W. (1999). In situ assembly of colloidal particles into miniaturized biosensors. *Langmuir* 15, 3693–3698. doi: 10.1021/la981729c

Wang, Y., Wei, W., Liu, X., and Zeng, X. (2009). Carbon nanotube/chitosan/gold nanoparticles-based glucose biosensor prepared by a layer-by-layer technique. *Mater. Sci. Eng. C* 29, 50–54. doi: 10.1016/j.msec.2008.05.005

Wang, J., Wu, Y., Zhou, P., Yang, W., Tao, H., Qiu, S., et al. (2018). A novel fluorescent aptasensor for ultrasensitive and selective detection of acetamiprid pesticide based on the inner filter effect between gold nanoparticles and carbon dots. *Analyst* 143, 5151–5160. doi: 10.1039/C8AN01166D

Wang, H., Wang, Y., Wang, W., Zhang, Y., Yuan, Q., and Tan, J. (2023). Materials-functionalized point-of-care testing devices for pathogen detection. *Acc. Mater Res.* 4, 1083–1094. doi: 10.1021/accountsmr.3c00151

Wang, Q., Wang, X., Gu, Q., and Guo, W. (2026). Conductive ternary MXene-noble metal nanocluster-protein composite hydrogel-based robust, anti-biofouling and ultrasensitive electrochemiluminescence platform for biothiol sensing. *Talanta* 299, 129046. doi: 10.1016/j.talanta.2025.129046

Wu, B., Hou, S., Xue, Y., and Chen, Z. (2018). Electrodeposition–assisted assembled multilayer films of gold nanoparticles and glucose oxidase onto polypyrrole-reduced graphene oxide matrix and their electrocatalytic activity toward glucose. *Nanomaterials* 8, 993. doi: 10.3390/nano8120993

Wu, X., Zhao, X., Zhao, X., Wang, J., Wang, S., and Zhang, Y. (2025). Machine-learning-assisted surface-enhanced raman spectroscopy for detecting phenolic antioxidants in oils using Ag@ZnO/g-C_3N_4 nanocomposites. *J. Food Compos. Analysis* 148, 108650. doi: 10.1016/j.jfca.2025.108650

Xiu, Z., Zhang, Q., Puppala, H. L., Colvin, V. L., and Alvarez, P. J. J. (2012). Negligible particle-specific antibacterial activity of silver nanoparticles. *Nano Lett.* 12, 4271–4275. doi: 10.1021/nl301934w

Xu, Y., Hu, C., and Hu, S. (2010). A reagentless nitric oxide biosensor based on the direct electrochemistry of hemoglobin adsorbed on The Gold colloids modified carbon paste electrode. *Sens. Actuators B Chem.* 148, 253–258. doi: 10.1016/j.snb.2010.05.028

Yang, T., Huang, H., Zhu, F., Lin, Q., Zhang, L., and Liu, J. (2016). Recent progresses in nanobiosensing for food safety analysis. *Sensors (Basel)* 16 (7), 1118. doi: 10.3390/s16071118

Yang, J., Yu, R., Zhang, W., Wang, Y., and Deng, Z. (2025). Electrochemical determination of creatinine based on multienzyme cascade-modified nafion/gold Nanoparticles/screen-printed carbon composite biosensors. *Sensors* 25, 4132. doi: 10.3390/s25134132

Yılmaz, D., Günaydın, B. N., and Yüce, M. (2022). Nanotechnology in food and water security: on-site detection of agricultural pollutants through surface-enhanced raman spectroscopy. *Emergent Mater* 5, 105–132. doi: 10.1007/s42247-022-00376-w

Yun, B. J., Kwon, J. E., Lee, K., and Koh, W.-G. (2019). Highly sensitive metal-enhanced fluorescence biosensor prepared on electrospun fibers decorated with silica-coated silver nanoparticles. *Sens. Actuators B Chem.* 284, 140–147. doi: 10.1016/j.snb.2018.12.096

Zakiyyah, S. N., Satriana, N. P., Fransisca, N., Gaffar, S., Syakir, N., Irkham, et al. (2025). Gold nanoparticle-modified screen-printed carbon electrodes for label-free detection of SARS-CoV-2 RNA using drop casting and spray coating methods. *ADMET DMPK* 13. 2577. doi: 10.5599/admet.2577

Zhang, Y., Zhang, Y., Zhou, W., He, P., Sun, X., Li, J., et al. (2024). Rapid and sensitive detection of SARS-CoV-2 IgM through luciferase luminescence on an automatic platform. *Int. J. Biol. Macromol.* 265, 130964. doi: 10.1016/j.ijbiomac.2024.130964

Zhao, W., Chiuman, W., Lam, J. C. F., McManus, S. A., Chen, W., Cui, Y., et al. (2008). DNA aptamer folding on gold nanoparticles: from colloid chemistry to biosensors. *J. Am. Chem. Soc.* 130, 3610–3618. doi: 10.1021/ja710241b

Zhao, Y., Han, J., Huang, J., Huang, Q., Tao, Y., Gu, R., et al. (2024). A miniprotein receptor electrochemical biosensor chip based on quantum dots. *Lab. Chip* 24, 1875–1886. doi: 10.1039/D3LC01100C

Zhao, X., Han, S., Chen, C., Lv, X., Li, J., and Chen, C. (2026). Deep learning-assisted SERS platform for label-free detection of celecoxib in serum using ag@pt@porous silicon bragg mirror composite substrate. *Spectrochim. Acta A Mol. Biomol. Spectrosc.* 348, 127165. doi: 10.1016/j.saa.2025.127165

Zhu, F., Zhao, G., and Dou, W. (2018). A non-enzymatic electrochemical immunoassay for quantitative detection of *Escherichia coli* O157:H7 using au@Pt and graphene. *Anal. Biochem.* 559, 34–43. doi: 10.1016/j.ab.2018.08.016

Zikulnig, J., Carrara, S., and Kosel, J. (2025). A life cycle assessment approach to minimize environmental impact for sustainable printed sensors. *Sci. Rep.* 15, 10866. doi: 10.1038/s41598-025-95682-8